The quasi-stationary state approximation to coupled mass transport and fluid-rock interaction in a porous medium

Article *in* Geochimica et Cosmochimica Acta · January 1988

DOI: 10.1016/0016-7037(88)90063-4

CITATIONS
327

READS
225

1 author:

Peter Lichtner
University of New Mexico
154 PUBLICATIONS **3,698** CITATIONS

SEE PROFILE

Geochimica et Cosmochimica Acta Vol. 52, pp. 143–165

0016-7037/88/$3.00 + .00

The quasi-stationary state approximation to coupled mass transport and fluid-rock interaction in a porous medium

PETER C. LICHTNER*
Department of Geology and Geophysics, University of California, Berkeley, CA 94720, U.S.A.

(*Received April* 3, 1987; *accepted in revised form October* 15, 1987)

Abstract—The quasi-stationary state approximation to mass transport and fluid-rock interaction provides a quantitative description of metasomatic processes over geologically significant time spans. The time evolution of a geochemical system within the quasi-stationary state approximation is represented by a sequence of stationary states. Each stationary state describes the fluid composition and rates of reacting minerals as a function of distance corresponding to a particular state of alteration of the host rock. Because time steps separating stationary states are not restricted by stability and accuracy requirements as apply to conventional finite difference algorithms, geologic time spans are attainable for complex geochemical systems. The approximation is valid if mineral reaction zone boundaries, surface area, porosity and permeability change slowly compared to the time required to establish a stationary state. The propagation in time of mineral alteration zones can be predicted without any additional assumptions of the functional relationship of the zone boundaries on time. Pure advective mass transport within the quasi-stationary state approximation is equivalent to a multiple reaction path description of combined fluid flow and chemical reaction based on a Lagrangian reference frame. The validity of the quasi-stationary state approximation is examined for reaction of the minerals calcite and quartz. An exact expression is obtained for the velocity and position of the dissolution front formed in a single component system for a linear kinetic rate law. Under certain conditions the velocity of the front is independent of the reaction rate constant and surface area and equal to the local equilibrium result. The mineral volume fraction profile depends linearly on the rate constant and surface area in the vicinity of the front. Numerical and analytical examples for the dissolution of quartz at 550°C and 1 kb are in excellent agreement with numerical finite difference calculations based on exact transient mass conservation equations. Finally, the quasi-stationary state approximation is applied to the hydrochemical weathering of K-feldspar resulting from infiltrating rainwater. Product minerals gibbsite, kaolinite and muscovite form alteration zones which propagate with time in response to the reduction in surface area and, eventually, complete reaction of the dissolving K-feldspar mineral grains. During the initial stages of alteration gibbsite forms directly from K-feldspar, but in later stages forms indirectly from kaolinite.

1. INTRODUCTION

THE ABILITY TO integrate equations governing geochemical processes in natural systems over time spans of geologic significance is essential for a quantitative description of mass transport coupled to fluid-rock interaction. In many cases usual finite difference techniques are limited to relatively short time spans as a result of the stringent requirements imposed by stability and accuracy considerations restricting the size of the allowable time step used in such algorithms. The situation is further complicated by the presence of mineral reaction zones which propagate with time leading to a Stefan or moving boundary problem. The zone boundaries are marked by sharp reaction fronts where rapid changes occur in fluid composition and mineral reaction rates, further restricting the size of the time step. This work investigates the ability of the quasi-stationary state approximation to fluid-rock interaction and mass transport to overcome these difficulties without loss in accuracy or numerical stability.

The quasi-stationary state approximation represents the time evolution of geochemical processes involving advective, diffusive and dispersive mass transport by a sequence of stationary states. Each stationary state represents the fluid composition and rates of reacting minerals as a function of distance for a particular state of alteration of the host rock. Within the quasi-stationary state approximation, fluid composition and mineral reaction rates adjust quasi-statically to changes in the host rock as it is progressively altered with time. The propagation in time of mineral alteration zones can be predicted without any additional assumptions of the functional relationship of the zone boundaries on time.

Because the time steps separating stationary states are not restricted by the stability and accuracy requirements applicable to conventional finite difference algorithms, geologically significant time spans are attainable for complex systems. In contrast, the size of the time step relating one stationary state to the next is governed by changes in the positions of mineral reaction zones, surface area, porosity and permeability. It is the rate at which these quantities change which determines the lifetime of each stationary state. Provided alteration of the host rock occurs sufficiently slowly compared to the time required to form a stationary state, the quasi-stationary state approximation is expected to be valid.

The use of the quasi-stationary approximation to describe metasomatic processes is not new. FRANTZ and MAO (1976, 1979) and WEARE *et al.* (1976) have previously used this approach, together with the assumption of local equilibrium between fluid and minerals, to describe mineral alteration resulting from diffusion and advection. These authors, however, assumed that the fluid composition formed an invariant point at reaction zone boundaries, an assumption which is not generally valid (LICHTNER *et al.*, 1986b). The current formulation differs from these studies in that minerals are assumed to react irreversibly with the fluid according to some prescribed kinetic rate law. Local equilibrium is recovered in the limit as the product of the rate constant and surface area tend towards infinity (LICHTNER, 1985). More recent

* *Present address:* Universität Bern, Mineralogisch-petrographisches Institut, Baltzer-Strasse 1, CH-3012 Bern, Switzerland.

applications of the quasi-stationary state approximation to metasomatic processes can be found in DOBROVOLSKY (1987), LICHTNER (1987), and ORTOLEVA *et al.* (1987), and references therein. The method has also been used to solve moving boundary problems involving heat transfer in which melting or solidification takes place (CARSLAW and JAEGER, 1959; RUBINSTEIN, 1971; LUNARDINI, 1981; CRANK, 1984; ARONSSON, 1985). In such cases the quasi-stationary state approximation is valid if the latent heat of fusion is much larger than the heat capacity of the liquid or solid phase.

The term "stationary" is used throughout this work rather than "steady" to emphasize that stationary states correspond to fixed boundaries of mineral alteration zones as well as other properties of the host rock including surface area, porosity and permeability. The term "steady" is reserved for properties that may vary in time but do so at a constant rate. One may note that the quasi-stationary state approximation is analogous to the adiabatic approximation describing the motion of electrons and nuclei in crystals and molecules, also referred to as the Born-Oppenheimer approximation (see, *e.g.*, BORN and HUANG, 1954). In this approximation the motion of electrons is presumed to follow the heavier and much slower-moving nuclei.

The paper is divided into three sections. The first considers the mathematical formulation of the quasi-stationary state approximation from the corresponding exact transient description based on the continuum theory of mixtures. All simplifications of porous media inherent in this theory apply also, of course, to the quasi-stationary state approximation. This section is followed by a section devoted to a single component system in which comparisons, both numerical and analytical, are made with the exact transient description. The paper concludes with an application of the quasi-stationary state approximation to weathering of a porous rock consisting of K-feldspar and quartz as rainwater percolates through the pores.

2. THE QUASI-STATIONARY STATE APPROXIMATION

The quasi-stationary state approximation to coupled mass transport and fluid-rock interaction is based on the assumption that fluid composition and mineral reaction rates adjust quasi-statically to changes in the state of alteration of the host rock. In a continuum based description of fluid-rock interaction, this includes changes with distance and time in mineral abundances, surface area, porosity and permeability and changes in the positions of reaction zone boundaries. The time evolution of a geochemical system in this approximation is represented by a sequence of stationary states. Each stationary state represents the fluid composition and mineral reaction rates corresponding to a particular spatial configuration of the host rock. Mineral abundances, boundaries of mineral alteration zones, porosity, permeability, and surface area of the reacting minerals are presumed to vary slowly compared to the time required to form a stationary state. The basis for the quasi-stationary state approximation is the observation that within a representative elemental volume the aqueous concentration of any particular species is generally much less than its concentration in minerals (FRANTZ and MAO, 1976, 1979; WEARE *et al.*, 1976).

To investigate qualitatively the quasi-stationary state approximation, it is instructive to consider a purely advective system from the point of view of a reference frame fixed with respect to the fluid, referred to as a Lagrangian frame of reference (BEAR, 1972). For definiteness consider the weathering of a porous rock, which for simplicity is assumed to consist entirely of K-feldspar, as rainwater percolates through the rock at a constant flow rate. Under appropriate pH conditions, reaction zones corresponding to product minerals gibbsite and kaolinite are formed as K-feldspar dissolves. The evolution with time of the spatial distribution of mineral alteration products can be obtained by considering a series of fluid packets as depicted schematically in Fig. 1. Each packet represents a closed system with respect to the fluid phase. With respect to the reacting minerals, however, the packets form an open system. The first packet of fluid deposits a sequence of product minerals along the flow path as it reacts with K-feldspar consisting of gibbsite followed by kaolinite (Fig. 1b). The widths of the alteration zones are determined by the amount of time the fluid in the packet reacts with K-feldspar as it traverses the flow path. Eventually the fluid in the packet must come to equilibrium with respect to K-feldspar after a sufficiently long travel distance. The initial abundance of K-feldspar remains virtually unchanged by the passage of a single packet, and hence the porosity, permeability and surface area of the K-feldspar are also unchanged.

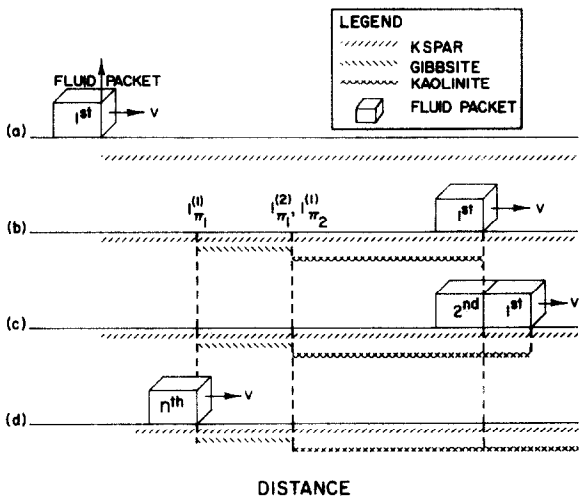

FIG. 1. Schematic illustration of the Lagrangian formulation of the quasi-stationary state approximation for the reaction of a hypothetical rock consisting of K-feldspar with infiltrating rainwater. (a) The first packet of infiltrating fluid enters a porous rock column consisting of an aqueous solution in equilibrium with K-feldspar. (b) As the packet moves downstream, the original fluid is displaced leaving behind reaction zones of gibbsite and kaolinite (see figure legend). The kaolinite zone grows linearly with time, while the gibbsite zone is stationary. (c) The second and subsequent fluid packets trace out identical reaction paths as the first packet provided significant changes in the volume fractions of the reacting minerals, surface area, permeability and porosity do not occur. (d) K-feldspar dissolves at the inlet leaving the next fluid packet undersaturated with respect to gibbsite when it reaches the previously deposited gibbsite zone. As a consequence gibbsite dissolves at the upstream end of the gibbsite zone and precipitates further downstream. Similar effects can also occur as a result of changes in surface area of the reacting minerals.

The question arises as to how the various alteration products deposited by one packet influence subsequent packets. Consider the second packet of fluid. Because its reaction path is identical to that of the first packet by assumption that the first packet did not significantly alter the dissolving K-feldspar, it must behave in an identical fashion as the first packet. Thus, as it arrives at the gibbsite zone deposited by the first packet, it must also become saturated with respect to gibbsite and continue to precipitate gibbsite further downstream until the kaolinite zone is reached. At this point the packet becomes saturated with respect to kaolinite. Consequently, the second packet merely adds to the already existing alteration zones produced by the first packet *at the same positions* along the flow path (Fig. 1c). Therefore, provided the surface area, porosity and permeability of the host rock remain unchanged, alteration products deposited by previous packets do not influence the reaction path of subsequent packets, which therefore follow the same reaction path as that of the very first packet. Thus, with the exception of reaction zones which end at the first packet and therefore advance downstream at the pore velocity, the positions of the mineral alteration zones are constant in time. In the example given here, the gibbsite zone is stationary while the downstream kaolinite zone moves with the fluid velocity. With the exception of the advancing front, this situation represents a stationary state in which the fluid composition and mineral reaction rates are constant in time. It turns out that the advancing front is actually of little practical importance because the fluid in this region is very close to equilibrium with respect to the host rock and therefore very little reaction occurs.

Clearly this stationary state condition cannot last indefinitely. As minerals in the host rock begin to completely dissolve (Fig. 1d), or significant changes occur in the porosity, permeability or surface area of the reacting minerals, the reaction zones must readjust to the altered reaction and fluid flow rates. This produces a new stationary state reaction path. In this case previously deposited product minerals now begin to play a role in the determination of the composition of subsequent fluid packets and their reaction products. Thus, for example, referring to Fig. 1d, when K-feldspar completely dissolves at the inlet to the porous column, the previously deposited gibbsite zone is no longer stable and it begins to dissolve at one end and precipitate further downstream. In general a particular stationary state reaction path persists until complete dissolution of a mineral occurs, or until significant changes occur in the porosity, permeability and mineral surface area. Note that a *change* in rock properties or fluid velocity is required to change the width of reaction zones in the stationary state regime.

Transient formulation

The mathematical formulation of the quasi-stationary state approximation follows from the corresponding transient description (see, *e.g.*, LICHTNER, 1985). The following development is based on a continuum representation of mass transport in a porous medium involving a multicomponent system of reacting minerals and fluid. Homogeneous reactions between aqueous species are assumed to be sufficiently rapid to maintain local equilibrium within the fluid phase. In contrast, heterogeneous reactions involving minerals and fluid are described through irreversible kinetic rate laws of which local equilibrium is a special case.

For the purpose of simplifying the resulting equations, it is useful to rearrange the chemical reactions occurring in the system into a particular canonical form (LICHTNER, 1985). Without loss in generality it can be shown that they can always be written with unit stoichiometric coefficients corresponding to aqueous complexes and minerals according to:

$$\sum_{j=1}^{N} \nu_{ji} \mathrm{A}_j \rightleftarrows \mathrm{A}_i, \tag{1}$$

and

$$\sum_{j=1}^{N} \nu_{jr} \mathrm{A}_j \rightleftarrows \mathrm{A}_r, \tag{2}$$

where the first set of reactions refer to homogeneous reactions within the fluid phase and the second set to heterogeneous reactions between fluid and minerals. The aqueous species denoted by the symbols $\{\mathrm{A}_j\}$ $(j = 1, \ldots, N)$, and all irreversibly reacting minerals, denoted by the symbols $\{\mathrm{A}_r\}$ $(r = 1, \ldots, M)$, are referred to as primary species. Aqueous complexes, designated by the symbol A_i, are referred to as secondary species. Unless otherwise indicated, the subscript i is reserved exclusively for these species. The quantities ν_{ji} and ν_{jr} denote the respective stoichiometric reaction matrices.

With this representation of the chemical reactions in the system, continuum mass conservation equations for the primary species can be expressed as the following system of $N + M$ coupled, nonlinear partial differential equations (LICHTNER, 1985):

$$\frac{\partial}{\partial t}(\phi \Psi_j) + \nabla \cdot \Omega_j = -\sum_{r=1}^{M} \nu_{jr} \frac{\partial \Xi_r}{\partial t} \quad (j = 1, \ldots, N), \tag{3}$$

and

$$\frac{\partial}{\partial t}(\phi_r \bar{V}_r^{-1}) = \frac{\partial \Xi_r}{\partial t} \quad (r = 1, \ldots, M), \tag{4}$$

where the first set of equations refers to aqueous species, and the second set to minerals. In these equations ϕ denotes the porosity of the porous medium, ϕ_r and Ξ_r denote the volume fraction and reaction progress density, respectively, of the rth mineral with molar volume $\bar{V}_r$, and the quantities Ψ_j and Ω_j are referred to as the generalized concentration and generalized flux respectively of the jth primary species. The right hand sides of Eqns. (3) and (4) represent source/sink terms describing the irreversible reaction of minerals and fluid with reaction rates $\partial \Xi_r / \partial t$. The generalized concentration Ψ_j is defined at position $\mathbf{r}$ and time t according to the expression

$$\Psi_j(\mathbf{r}, t) = C_j(\mathbf{r}, t) + \sum_i \nu_{ji} C_i(\mathbf{r}, t), \tag{5}$$

where $C_j(\mathbf{r}, t)$ refers to the concentration of the jth primary species, and the sum runs over all aqueous secondary species with concentration $C_i(\mathbf{r}, t)$ related to the concentrations of the primary species through the mass action equation

$$C_i(\mathbf{r}, t) = K_i \gamma_i^{-1}(\mathbf{r}, t) \prod_{j=1}^{N} (\gamma_j(\mathbf{r}, t) C_j(\mathbf{r}, t))^{\nu_{ji}}, \tag{6}$$

where $\gamma_l(\mathbf{r}, t)$ denotes the activity coefficient of the lth primary or secondary aqueous species and K_i denotes the corresponding equilibrium constant. The generalized flux Ω_j is defined by the expression

$$\Omega_j(\mathbf{r}, t) = \mathbf{J}_j(\mathbf{r}, t) + \sum_i \nu_{ji} \mathbf{J}_i(\mathbf{r}, t), \tag{7}$$

where the fluid flux of the lth species $\mathbf{J}_l(\mathbf{r}, t)$ is given by a sum of contributions from diffusive and advective fluxes according to

$$\mathbf{J}_l(\mathbf{r}, t) = -\phi(\mathbf{r}, t) \sum_k D_{lk}(\mathbf{r}, t) \nabla C_k(\mathbf{r}, t) + v(\mathbf{r}, t) C_l(\mathbf{r}, t), \tag{8}$$

where the sum is over both primary and secondary aqueous species, D_{lk} denotes the diffusion coefficient matrix and v denotes the fluid Darcy velocity. The term "generalized" is used to refer to the quan-

tities Ψ_j and Ω_j since they may have no direct physical meaning. For the case in which the stoichiometric coefficients v_{ji} are all positive, the generalized concentration Ψ_j coincides with the total concentration of that species and Ω_j to the corresponding total flux. However, for species such as H^+, Ψ_{H^+} may take on negative values (LICHTNER, 1985).

Conservation of volume relates the porosity to the sum of the mineral volume fractions according to the expression

$$\phi(\mathbf{r},t)+\sum_{r=1}^{M}\phi_r(\mathbf{r},t)=\phi_R, \tag{9}$$

where ϕ_R denotes the total reactive volume fraction occupied by minerals and fluid. The total reactive volume fraction is less than or equal to one. A value for ϕ_R less than one provides for the presence of isolated pore spaces which are not part of the flow porosity, as well as inert rock which does not come in contact with the fluid as, for example, may be caused by armouring effects.

The requirement that the only admissible solutions to the mass conservation equations are those for which the mineral volume fractions ϕ_r satisfy the inequality

$$0\le\phi_r(\mathbf{r},t)\le\phi_R, \tag{10}$$

defines a moving boundary problem in which the spatial region occupied by mineral A_r in general varies with time. This condition complicates the solution to the mass transport equations. By taking into account the presence of mineral alteration zones, the reaction rate $\partial\Xi_r/\partial t$ can be written in the form

$$\frac{\partial\Xi_r}{\partial t}(\mathbf{r},t)=\zeta_r(\mathbf{r},t)I_r(\mathbf{r},t), \tag{11}$$

where $I_r(\mathbf{r}, t)$ designates the actual rate of reaction, and the function $\zeta_r(\mathbf{r}, t)$, defined below, accounts for the presence of mineral A_r in the representative elemental volume located at position $\mathbf{r}$. One possible form of I_r based on transition state theory (HELGESON *et al.*, 1984; LASAGA, 1984) is given by the expression

$$I_r(\mathbf{r},t)=\alpha_r(\mathbf{r},t)k_r^f\{Q_r(\mathbf{r},t)-K_r^{-1}\}, \tag{12}$$

where $\alpha_r(\mathbf{r}, t)$ denotes the surface area of the rth mineral per unit volume of bulk porous medium, K_r denotes the equilibrium constant, k_r^f denotes the rate constant for the forward reaction as written in Eqn. (2), and Q_r denotes the activity product defined by

$$Q_r(\mathbf{r},t)=\prod_{j=1}^{N}(a_j(\mathbf{r},t))^{\nu_{jr}}, \tag{13}$$

where a_j denotes the activity of the jth primary species. The function $\zeta_r(\mathbf{r}, t)$ is defined as unity either if the rth mineral is present within the representative elemental volume located at position $\mathbf{r}$, or if $\phi_r(\mathbf{r}, t) = 0$ but $I_r(\mathbf{r}, t) > 0$ indicating the onset of precipitation. Otherwise ζ_r has the value zero. Thus $\zeta_r(\mathbf{r}, t)$ can be expressed in symbols as

$$\zeta_r(\mathbf{r},t)=\begin{cases}1 & (\phi_r(\mathbf{r},t)\neq 0,\ \text{or}\ \phi_r(\mathbf{r},t)=0\ \text{and}\ I_r(\mathbf{r},t)>0)\\ 0 & (\text{otherwise})\end{cases}. \tag{14}$$

According to the definitions above, the reaction rate $I_r(\mathbf{r}, t)$ is positive for precipitation, $Q_r(\mathbf{r}, t) > K_r^{-1}$, and negative for dissolution, $Q_r(\mathbf{r}, t) < K_r^{-1}$. For $Q_r = K_r^{-1}$ the rate vanishes and equilibrium is obtained. Local equilibrium is obtained in the limit as the product of the rate constant and surface area tend towards infinity. As a consequence, $Q_r \to K_r^{-1}$, resulting in an indeterminate value for the reaction rate: $\infty \cdot 0$.

The description of the transient problem is completed by specifying appropriate initial and boundary conditions. These may be given, for example, by specifying the initial generalized concentration Ψ_j^∞ and mineral volume fraction ϕ_r^∞ at $t = 0$ as functions of distance, and the generalized solute flux Ω_j^0 or concentration Ψ_j^0 at the inlet to the porous column as prescribed functions of time.

Under conditions that changes in surface area, porosity and permeability are negligible, Eqns. (3) and (4) decouple and may be solved independently of each other. Generally this separation of the transport equations is valid only for time scales that are much shorter than the time for a mineral grain to completely dissolve, or the time required for significant changes to occur in the reacting surface area, porosity, or permeability. Otherwise the equations are coupled. In either case their solution can be prohibitively time consuming, especially for many component systems.

Stationary states

The quasi-stationary state approximation follows from the transient description of the mass transport equations by neglecting the first term on the left-hand side of Eqn. (3) containing the partial time derivative $\partial(\phi\Psi_j)/\partial t$. This results in the following system of partial differential equations in the space coordinate $\mathbf{r}$ for the concentrations of the solute species

$$\nabla\cdot\Omega_j=-\sum_r\nu_{jr}\frac{\partial\Xi_r}{\partial t}\quad(j=1,\ldots,N). \tag{15}$$

These equations must be solved subject to appropriate boundary conditions at the inlet and outlet to the porous medium, and continuity conditions of the concentration and flux across each reaction front. For systems with a single spatial dimension the latter conditions can be expressed in the form

$$[\Psi_j]_{l_r}=\Psi_j^{(-)}(l_r)-\Psi_j^{(+)}(l_r)=0, \tag{16}$$

and

$$[\Omega_j]_{l_r}=\Omega_j^{(-)}(l_r)-\Omega_j^{(+)}(l_r)=0, \tag{17}$$

where the square brackets $[\ldots]_{l_r}$ denote the jump in the enclosed quantity across the reaction front l_r, and the superscript $(+)$ designates approaching the reaction front from the right and $(-)$ from the left. A solution to Eqn. (15) subject to Eqns. (16) and (17) defines a stationary state. It provides the concentrations of the solute species and mineral reaction rates as functions of distance for fixed values of the mineral zone boundaries, surface area, porosity and permeability. These equations are far simpler to solve than the original partial differential equations for the transient case given by Eqn. (3).

A stationary state may be thought of as the open system analogue of an equilibrium state corresponding to a closed system (DENBIGH, 1951). Both are independent of time. Furthermore, an equilibrium state is a special case of a stationary state corresponding to the limiting case in which the flux of matter or heat into the system vanishes. A stationary state, however, is generally not in equilibrium. A stationary state configuration corresponding to an interacting system of chemical species undergoing advective, diffusive or dispersive mass transport, is a function of the porosity, permeability, surface area of each reacting mineral, and the function $\zeta_r(\mathbf{r}, t)$ defined in Eqn. (14), specifying the region of space each mineral occupies. Under certain simplifying assumptions, the mineral volume fractions $\{\phi_r(\mathbf{r}, t)\}$ serve to completely determine the properties of the host rock as functions of distance and time. Total rock porosity is related to the mineral volume

fractions according to the volume conservation equation given by Eqn. (9). The functional dependence of flow or connected porosity, as well as surface area and permeability is more difficult to determine, however, and generally must be based on phenomenological relationships. From geometrical considerations the surface area per unit volume of bulk porous medium of the rth mineral α_r can be argued to vary according to the two thirds power of the mineral volume fraction ϕ_r according to

$$\alpha_r(\mathbf{r}, t) = \alpha_r^{\infty} \left\{ \frac{\phi_r(\mathbf{r}, t)}{\phi_r^{\infty}} \right\}^{2/3}, \tag{18}$$

where α_r^{∞} and ϕ_r^{∞} denote the initial surface area and volume fraction, respectively, at $t = 0$. However, it should be noted that in general the surface area need not be so simply related to mineral abundance, but may also be a function of the surface roughness which may increase or decrease with the degree of reaction. A proper characterization of the permeability, and tortuosity in the case of diffusional mass transport, would, in principle, require knowledge of mineral textures in addition to their abundances. One empirical constitutive relation often used in practical calculations, the Carman-Kozeny equation, represents the permeability as a power function of porosity (BEAR, 1972). In the following it is presumed that the mineral volume fractions completely characterize the host rock as it evolves in time. For such circumstances, the stationary state representation of the concentration of the jth primary species can be expressed as a function of the form $C_j(\mathbf{r}; \{\phi_r\})$. Likewise the reaction rate has the form $I_r(\mathbf{r}; \{\phi_r\})$.

For the case of advective and diffusive mass transport with a diagonal solute diffusion coefficient matrix consisting of equal and constant elements denoted by D, and constant flow velocity v, the stationary state equations for a one-dimensional system are given by

$$D\frac{d^2\Psi_j}{dx^2} - \frac{v}{\phi}\frac{d\Psi_j}{dx} = \frac{1}{\phi}\sum_r \nu_{jr}\frac{\partial \Xi_r}{\partial t}(x; \{\phi_r\}). \tag{19}$$

These equations represent a set of coupled, second order, ordinary differential equations for the stationary states $C_j(x; \{\phi_r\})$. In general they are non-linear as a result of the kinetic rate term on the right-hand side, according to Eqn. (12). Solutions to Eqn. (19) are subject to continuity conditions at reaction zone boundaries expressed by Eqns. (16) and (17).

Lagrangian representation. The stationary state equations take a particularly simple form for constant pure advective fluid flow discussed qualitatively at the beginning of this section. For one-dimensional transport a stationary state satisfies the following set of first order ordinary differential equations

$$v\frac{d\Psi_j}{dx} = -\sum_r \nu_{jr}\frac{\partial \Xi_r}{\partial t}(x; \{\phi_r\}). \tag{20}$$

For this case the continuity conditions expressed by Eqns. (16) and (17) are equivalent. Relating distance along the flow path to the travel time denoted by t' according to

$$\frac{dx}{dt'} = \frac{v}{\phi}, \tag{21}$$

or, in the case of constant porosity and Darcy flow velocity, by the integrated form

$$x = \frac{vt'}{\phi}, \tag{22}$$

the stationary state equations for pure advective transport become, in either case,

$$\phi\frac{d\Psi_j}{dt'} = -\sum_r \nu_{jr}\frac{\partial \Xi_r}{\partial t}(t'; \{\phi_r\}), \tag{23}$$

where the time t' is introduced as the independent variable. These equations represent a Lagrangian formulation of coupled fluid flow and fluid-rock interaction (LICHTNER *et al.*, 1986c, 1987). Equations (21) or (22) represent the Lagrangian equation of motion for the center of mass of a fluid packet. The chemical composition of the packet is parameterized by the time t' that the packet is in contact with the host rock. Mineral products precipitated from the packet are left behind as the packet advances downstream. They do not back react with the fluid in the packet in contrast to aqueous reaction products resulting from a mineral dissolving into solution, which are carried along by the packet. Hence the fluid packet is open with respect to minerals which, from the point of view of an observer at rest with respect to the packet, continuously enter and exit from the packet. The packet is presumed closed with respect to transfer of matter within the fluid phase, implying that diffusive and dispersive fluxes are negligible compared to advective mass transfer. Because each stationary state solution to Eqn. (23) corresponds to a different reaction path traced out by the packet fluid composition in activity space, the Lagrangian formulation is also referred to as the multiple reaction path formulation (LICHTNER *et al.*, 1986c). Equations for a single reaction path were developed by HELGESON (1968) and later extended by HELGESON and MURPHY (1983) to include the irreversible reaction of minerals described by a kinetic rate law. The single reaction path method has been extensively applied to many geochemical systems.

A solution to Eqn. (23) yields the concentrations of the aqueous species and mineral reaction rates as a function of elapsed time, or equivalently, of the position of the packet along the flow path, as obtained from Eqn. (21) or (22). Transforming the solution $C_j(t'; \{\phi_r\})$ to Eqn. (23) with the inverse of Eqn. (22), or the inverse of the integrated form of Eqn. (21) in the case of a time-dependent flow velocity, results in the following expression for the concentration $C_j(x; \{\phi_r\})$ as a function of distance along the flow path

$$C_j(x; \{\phi_r\}) = \begin{cases} C_j(\phi x/v; \{\phi_r\}) & (x \le vt'/\phi) \\ C_j^{\infty} & (x > vt'/\phi) \end{cases} \tag{24}$$

where C_j^{∞} denotes the initial composition of the fluid which is assumed to be in equilibrium with the host rock. Similarly the mineral reaction rate $\partial \Xi_r(t'; \{\phi_r\})/\partial t$ can be expressed as a function of distance according to:

$$\frac{\partial \Xi_r}{\partial t}(x; \{\phi_r\}) = \begin{cases} \dfrac{\partial \Xi_r}{\partial t}(\phi x/v; \{\phi_r\}) & (x \le vt'/\phi) \\ 0 & (x > vt'/\phi) \end{cases}. \tag{25}$$

Thus for times greater than $\phi x/v$, equal to the time required for the front of the infiltrating fluid to travel a distance x, stationary state representations of the concentrations and rates

of reacting minerals are obtained which are functions of distance only and not time.

For constant surface area and permeability, the fluid composition and location of mineral alteration zones are independent of porosity. This statement follows immediately from Eqn. (20) which only depends on the porosity of the porous medium through the surface area of the reacting minerals contained in the term involving the reaction rate on the right-hand side, and through the permeability which determines the flow velocity v. The width of a particular reaction zone within the Lagrangian representation can be determined by noting the times of appearance and disappearance of the corresponding mineral, and multiplying the difference in these times by the flow rate. Thus, if the fluid becomes saturated with respect to the rth mineral at time $\tau_r^{(1)}$, and the mineral stops precipitating at time $\tau_r^{(2)}$, the width of the corresponding reaction zone Δl_r is given by

$$\Delta l_r = \frac{v}{\phi}(\tau_r^{(2)} - \tau_r^{(1)}). \tag{26}$$

Although it may not be immediately apparent from this equation, Δl_r is independent of the porosity for constant surface area and permeability of the porous medium as already noted above. This is because the surface area of the reacting minerals in contact with the fluid packet, and hence the reaction rate, are inversely proportional to the porosity and thus $\tau_r^{(i)}$ is directly proportional to ϕ (LICHTNER *et al.*, 1986c, 1987). The ratio of the lengths of the reaction zones is independent of the flow velocity and equal to the ratio of times of duration of the zones. Since the length of each reaction zone is proportional to the duration of time the mineral is in contact with the fluid packet, an increase in the dissolution rate, for example, caused by increasing the temperature or surface area, results in a decrease in the width of the reaction zone.

Time evolution in the quasi-stationary state approximation

The time evolution of a geochemical system within the quasi-stationary state approximation is represented by a sequence of stationary states, each stationary state corresponding to a different degree of alteration of the reacting host rock. The volume fraction of the rth mineral at position $\mathbf{r}$ and time $t + \Delta t$, $\phi_r(\mathbf{r}, t + \Delta t)$, is determined from the stationary state at time t. Integrating Eqn. (4) at a fixed point in space, noting that the mineral reaction rate I_r is constant, results in a linear dependence of the volume fraction ϕ_r on time according to the expression

$$\phi_r(\mathbf{r}, t + \Delta t) = \phi_r(\mathbf{r}, t) + \bar{V}_r \zeta_r(\mathbf{r}; \{\phi_r\}) I_r(\mathbf{r}; \{\phi_r\}) \Delta t, \tag{27}$$

where $\phi_r(\mathbf{r}, t)$ denotes the mineral volume fraction at time t.

Once the mineral volume fractions have been determined at time $t + \Delta t$, the corresponding stationary state is obtained by solving Eqn. (15). Each stationary state must be consistent with Eqn. (10), specifying that the mineral volume fractions be positive or zero, resulting in altered positions of mineral reaction zones. In addition the stationary state corresponds to altered mineral surface areas, porosity, permeability and tortuosity. The above process may be repeated, in principle, indefinitely. The final result must, of course, be independent of the time step Δt. This procedure amounts to a finite difference algorithm in which the continuous evolution of the system with time is replaced by discrete time intervals Δt. Convergence is tested by varying the size of the time step Δt. The time step Δt represents the lifetime of the stationary state obtained at time t. The usefulness of the quasi-stationary state approximation rests on the rapid formation of a stationary state compared to its lifetime Δt. The lifetime of the stationary state is determined by several factors including changes in surface area, porosity and permeability, as well as complete dissolution of one of the minerals. In this latter case, the stationary state lifetime is given by

$$\Delta t_r = \frac{\phi_r(\mathbf{r}, t)}{\bar{V}_r |I_r|}, \tag{28}$$

corresponding to complete dissolution of the rth mineral at position $\mathbf{r}$. This result is used below to determine the time evolution, within the quasi-stationary state approximation, of a single component system involving the propagation of a mineral dissolution front.

3. SINGLE REACTING SOLUTE SPECIES WITH LINEAR KINETICS

To investigate further the quasi-stationary state approximation, it is instructive to consider a simple example involving the reaction of a hypothetical stoichiometric mineral A_s with solute species A according to

$$A \rightleftarrows A_s. \tag{29}$$

The reaction is assumed to proceed according to a linear kinetic rate law which may be expressed in the form

$$I_s = k_f \alpha [C - C_{eq}], \tag{30}$$

where k_f denotes the forward rate constant for the reaction as written above, α denotes the surface area per unit bulk volume of porous rock, C denotes the aqueous concentration of species A, and C_{eq} designates the concentration of species A in equilibrium with mineral A_s. A sufficiently dilute solution is assumed so that the activity coefficient can be set equal to unity. An example of such a reaction is the dissolution and precipitation of quartz.

At $t = 0$ a fluid undersaturated with respect to mineral A_s is allowed to infiltrate or diffuse into a porous medium with an initial volume fraction of mineral A_s equal to ϕ_s^∞ and with porosity ϕ as depicted in Fig. 2. The fluid originally present in the pore spaces is assumed to be in equilibrium with respect to the mineral. These statements are expressed mathematically by the initial conditions specified by

$$C(x, 0) = C_{eq}, \tag{31}$$

and

$$\phi_s(x, 0) = \phi_s^\infty, \tag{32}$$

and the boundary condition

$$C(0, t) = C_0, \tag{33}$$

where $C_0 < C_{eq}$ denotes the concentration of solute species A at the inlet, and ϕ_s denotes the mineral volume fraction.

For constant porosity of the porous medium transient mass

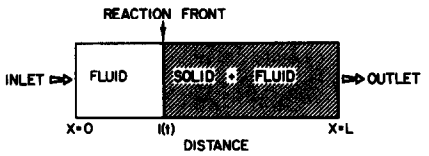

FIG. 2. Schematic diagram of a one-dimensional porous column consisting of a fluid reacting with a solid phase. A reaction front corresponding to complete dissolution of the solid is located at $l(t)$.

conservation equations for the solute species A and mineral A_s can be expressed in the form

$$D\frac{\partial^2 C}{\partial x^2}-\frac{v}{\phi}\frac{\partial C}{\partial x}-\frac{\partial C}{\partial t}=\frac{1}{\phi}\frac{\partial \Xi_s}{\partial t}, \tag{34}$$

for the solute concentration $C(x, t)$, and

$$\frac{\partial \phi_s}{\partial t}=\bar{V}_s\frac{\partial \Xi_s}{\partial t}, \tag{35}$$

for the mineral volume fraction $\phi_s(x, t)$, as follows from Eqns. (3) and (4), where $\partial \Xi_s/\partial t$ denotes the rate of reaction of mineral A_s with the fluid.

As the mineral reacts with the undersaturated fluid, a reaction front forms separating the porous medium into two regions. One region is occupied by the mineral, and in the other region the mineral has completely dissolved (see Fig. 2). In what follows the variation in porosity resulting from chemical reaction is not taken into account. The solution to the mass conservation equations must determine not only the solute concentration $C(x, t)$ and mineral volume fraction $\phi_s(x, t)$ as functions of distance and time, but also the position of the reaction front, denoted by $l(t)$. The requirement that the mineral volume fraction ϕ_s satisfy the inequality

$$0 \le \phi_s(x,t) \le 1, \tag{36}$$

defines a moving boundary problem in which the spatial region occupied by mineral A_s changes with time. The position of the mineral reaction front $l(t)$ is defined implicitly by the relation

$$\lim_{x \to l^+(t)} \phi_s(x,t)=0, \tag{37}$$

where the plus sign signifies that the boundary is to be approached from the side occupied by mineral A_s, assumed to be the region $x > l(t)$. Taking into account the position of the reaction front, the reaction rate may be expressed according to the equation

$$\frac{\partial \Xi_s}{\partial t}(x,t)=I_s(x,t)\theta(x-l(t)), \tag{38}$$

where I_s is given by Eqn. (30) and $\theta(x)$ denotes the Heaviside function defined by

$$\theta(x)=\begin{cases}1 & (x>0)\\ 0 & (x<0)\end{cases}. \tag{39}$$

The Heaviside function $\theta(x)$ corresponds to the function ζ_r defined in Eqn. (14).

Validity of the quasi-stationary state approximation

In the case of surface controlled dissolution, the appearance of the reaction front is delayed from the initial time of reaction of the undersaturated fluid with the mineral. This is in contrast with the situation of local equilibrium in which a sharp reaction front, referred to as a shock front, immediately forms (LICHTNER *et al.*, 1986a,b). The local equilibrium case is briefly reviewed in Appendix I for the case of pure advective mass transport. The time required for the mineral A_s to dissolve completely at the inlet to the porous column follows by integrating Eqn. (35) with the reaction rate given by Eqn. (38) evaluated at $x = 0$. For constant surface area this time, denoted by τ_0, is given by

$$\tau_0=\frac{\phi_s^\infty}{\bar{V}_s k_f \alpha \Delta C_0}, \tag{40}$$

with

$$\Delta C_0 = C_{eq}-C_0. \tag{41}$$

If the surface area is a function of the mineral volume fraction as expressed by Eqn. (18), the expression for τ_0 becomes multiplied by a factor of three as follows directly by integrating Eqn. (35). The delay time is inversely proportional to the rate constant, surface area, concentration difference, and mineral molar volume, and directly proportional to the initial mineral volume fraction. In the limit as the product $k_f\alpha$ tends to infinity, τ_0 vanishes and local equilibrium between the fluid and mineral is approached. The value of τ_0 may range over many orders of magnitude from hundreds of thousands of years to just seconds depending on the rate constant, surface area, initial mineral volume fraction, composition of the infiltrating fluid, mineral solubility and temperature.

For times earlier than τ_0 there exists an exact, analytical solution to the transient mass transport equations for the special assumptions of constant surface area, porosity, diffusivity and fluid flow velocity given by Eqn. (II.1) in Appendix II. In this case the mineral A_s has not completely dissolved at any point along the flow path and $l = 0$. The results presented in Appendix II demonstrate that a stationary state is formed during a characteristic time τ given by Eqn. (II.9). The condition for the validity of the quasi-stationary state approximation for the first reaction path is that the delay time τ_0 be much longer than the time τ required to establish a stationary state. Thus the ratio τ_0/τ must satisfy the inequality

$$\frac{\tau_0}{\tau}=\frac{\Lambda^2 v^2}{16\phi D k_f \alpha}\frac{\bar{V}_s^{-1}\phi_s^\infty}{\phi \Delta C_0} \gg 1, \tag{42a}$$

where the quantity Λ is defined by Eqn. (II.3). The value of the ratio depends on the temperature, pressure, fluid flow rate, diffusion coefficient, surface area, and the initial abundance of the reacting mineral. In the limit as the product of the rate constant and surface approach infinity, the ratio of τ_0/τ is proportional to the local equilibrium retardation factor of the dissolution front given by Eqn. (I.7) in Appendix I:

$$\lim_{k_f\alpha \to \infty}\frac{\tau_0}{\tau}=\frac{1}{4}\frac{\bar{V}_s^{-1}\phi_s^\infty}{\phi \Delta C_0}. \tag{42b}$$

In Fig. 3a estimates for the ratio τ_0/τ are plotted as a function of temperature for minerals quartz and calcite with the cor-

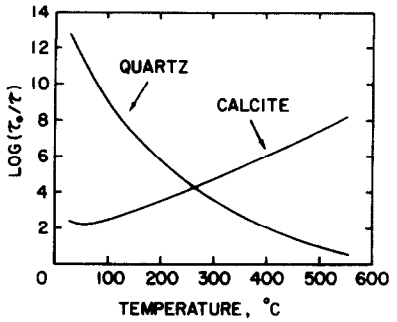

FIG. 3a. The ratio τ_0/τ plotted as a function of temperature at 1 kb for the minerals quartz and calcite. A value greater than one indicates validity of the quasi-stationary state approximation for the first stationary state. The retrograde solubility of calcite causes the ratio to increase with temperature in spite of the increase in the rate constant, while the ratio decreases for quartz because of its prograde solubility at 1 kb. The values used in the calculation for the various quantities entering Eqn. (42a) are given in the text and Fig. 3b.

responding values used for the rate constants and equilibrium constants shown in Fig. 3b. The rate constant for calcite was taken from SJÖBERG and RICKARD (1984) as modified by MURPHY *et al.* (1987), and that for quartz from RIMSTIDT and BARNES (1980). For both minerals the rate constant k_f may be represented in the form of a modified Arrhenius equation based on transition state theory given by (HELGESON *et al.*, 1984)

$$k_f = AKT \exp\left\{\frac{-\Delta H^{\ddagger}}{RT}\right\}, \tag{43}$$

where the enthalpy of activation $\Delta H^{\ddagger}$ has the values -18 and -8.4 kcal mole^{-1} and the logarithm of the pre-exponential factor A has the values -7.081 and -5.117 moles cm^{-2} sec^{-1} °K^{-1} for quartz and calcite, respectively. Equilibrium constants K were taken from the computer code SUPCRT corresponding to a pressure of 1 kb (BOWERS *et al.*, 1984, and references therein). A fluid flow rate of 1 m year, surface area of 10 cm^{-1} and initial volume fraction $\phi_s^{\infty} = 0.1$ were used. Values for the diffusion coefficient were adapted from OELKERS and HELGESON (1988), and range from 10^{-5} cm^2 sec^{-1} at 25°C to 10^{-3} cm^2 sec^{-1} at 600°C. In the case of calcite dissolution, the molalities of Ca^{2+} and CO_3^{2-} were taken to be identical, and the effects of pH and other carbonate species were ignored. The ratio τ_0/τ is found to decrease with increasing temperature for quartz, but increase for calcite as a consequence of its retrograde solubility. The quasi-stationary state approximation appears to be valid over the entire temperature range of 25–600°C for both minerals, despite their widely differing rate constants. It should be noted, however, that the curves shown in Figs. 3a and 3b represent an extrapolation of the available data for temperatures above approximately 300°C for quartz and 62°C for calcite, and should only be considered a rough estimate.

Exact solution to the quasi-stationary state equations

As discussed above, a solution to the equations representing the quasi-stationary state approximation is expressed as a sequence of stationary states, each stationary state corresponding to a different configuration of the host rock as it becomes altered with time. Mathematically, the quasi-stationary state solution for solute species A reacting with mineral A_s can be represented by the sequence of stationary states $\{C(x; l_1), C(x; l_2), \cdots\}$ for the solute concentrations corresponding to the reaction front of mineral A_s located at positions $\{l_1, l_2, \cdots\}$ at the discrete times $\{t_1, t_2, \cdots\}$. The first stationary state corresponds to $l_1 = 0$. For this stationary state $t_1 = \tau_0$, the time of first appearance of the front. The lifetime of the kth stationary state can be expressed as

$$\Delta t_k = t_{k+1} - t_k + \delta_{k1}\tau_0, \tag{44}$$

where δ_{k1} denotes the Kronecker delta function, with values equal to one if $k = l$ and zero otherwise. Note that the lifetime of the first stationary state is equal to t_2, the time at which the front advances to l_2 and a new stationary state is formed. The mineral volume fraction at time t_k and reaction front position l_k is denoted by $\Phi_s(x; l_k)$. By definition

$$\Phi_s(l_k; l_k) = 0, \tag{45}$$

with $\Phi_s(x; l_k) = 0$ for $x \le l_k$, and $\Phi_s(x; l_k) > 0$ for $x > l_k$. The problem is thus to determine the functional form of the quantities $C(x; l_k)$ and $\Phi_s(x; l_k)$, as well as the positions of the reaction front l_k and the associated times t_k for $k = 1, 2, \ldots$.

The differential equation for the stationary state $C(x; l)$ with the reaction front located at the position l has the form:

$$D\frac{d^2C}{dx^2} - \frac{v}{\phi}\frac{dC}{dx} = \frac{1}{\phi}I_s(x; l) \quad (x \ge l(t)),$$
$$= 0 \quad (x < l(t)), \tag{46}$$

Solutions to this equation for the cases of pure advection and diffusion, and combined advection-diffusion, satisfying the initial and boundary conditions given by Eqns. (31) and (33) and the continuity conditions given by Eqns. (16) and (17) are given in Appendix III. A fixed position of the reaction front l, constant surface area, porosity, diffusivity and fluid flow velocity is assumed. According to Appendix III, for $x \ge l$, $C(x; l)$ has the form

$$C(x; l) = C_{eq} - (C_{eq} - C_l)e^{-q(x-l)}, \tag{47}$$

where C_l denotes the concentration at the reaction front l, and the quantity q is defined by

$$q = \begin{cases} \dfrac{k_f\alpha}{v} & (D = 0, v \ne 0) \quad (48a) \\ (k_f\alpha/\phi D)^{1/2} & (D \ne 0, v = 0), \quad (48b) \\ \dfrac{v}{2\phi D}(\Lambda - 1) & (D \ne 0, v \ne 0) \quad (48c) \end{cases}$$

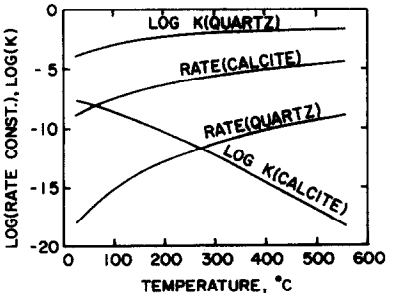

FIG. 3b. Logarithm of rate constants and equilibrium constants for minerals quartz and calcite plotted as a function of temperature as used in Fig. 3a. The equilibrium constants correspond to a pressure of 1 kb. The rate constants are obtained from Eqn. (43) with parameters given in the text.

for the respective cases of pure advection, pure diffusion, and combined advection-diffusion. Explicit expressions for C_l are given in Appendix III. The quantity Λ is defined by

$$\Lambda = \left[1 + \frac{4\phi D k_f \alpha}{v^2}\right]^{1/2}. \tag{49}$$

Thus each stationary state has the particularly simple form of a function exponentially decaying with distance from the reaction front. The characteristic length q^{-1} provides a measure of the approximate distance from the reaction front at which equilibrium of the fluid with mineral A_s is obtained. The corresponding stationary state dissolution rate is given as a function of distance for $x \geq l$ by the expression

$$I_s(x; l) = -k_f \alpha \Delta C_l e^{-q(x-l)}, \tag{50}$$

with

$$\Delta C_l = C_{eq} - C_l, \tag{51}$$

as follows from Eqn. (30). The dissolution rate is most rapid at the reaction front where the mineral is farthest from equilibrium, and diminishes exponentially away from the front as the fluid composition approaches equilibrium with the mineral.

For times $t \leq \tau_0$ an explicit expression for the volume fraction $\phi_s(x, t)$ can be obtained by integrating Eqn. (35), using Eqns. (30) and (38) with $l = 0$ to give:

$$\phi_s(x, t) = \phi_s^\infty \left(1 - \frac{t}{\tau_0} e^{-qx}\right), \tag{52a}$$

where the delay time τ_0 has been introduced from Eqn. (40). At each point x in space, the ϕ_s decreases linearly with time, eventually becoming zero at the inlet at $t = \tau_0$. According to this result, it follows that

$$\Phi_s(x; l = 0) = \phi_s^\infty (1 - e^{-qx}). \tag{52b}$$

For $t > \tau_0$ the dissolution front $l(t) > 0$ forms, which propagates at a retarded velocity compared to the velocity of some inert solute species. In this case the quasi-stationary state approximation also yields an analytical solution for the mineral volume fraction and solute concentration as functions of time and distance, as well as the position and velocity of propagation of the reaction front as a function of time. To determine explicit representations for the functions $C(x; l)$, $\Phi_s(x; l)$ and $l(t)$, assume that the reaction front has advanced to the position l in time t_l, and consider the displacement of the front through a distance Δl in time Δt_l. As a result a new stationary state is formed corresponding to the front located at $l + \Delta l$ and time $t + \Delta t_l$. Then the solute concentration for $x \geq l(t)$ is represented by the stationary state $C(x; l)$ given in Eqn. (47) with reaction rate given by Eqn. (50). Here l corresponds to any one of the l_k labeling the sequence of stationary states. Integrating Eqn. (35) with the boundary condition that the mineral volume fraction vanish at $x = l$ and $t = t_l$ gives:

$$\phi_s(x, t) = \Phi_s(x; l) - (t - t_l) \bar{V}_s k_f \alpha \Delta C_l e^{-q(x-l)}, \tag{53}$$

where $\Phi_s(x; l)$ denote the mineral volume fraction at time t_l with the position of the reaction front located at $x = l$ (recall that $\Phi_s(l; l) = 0$ by definition). This relation is valid for $x \geq l$ and $t \geq t_l$, but less than or equal to the time required for the mineral to completely dissolve at $x = l + \Delta l$, for $\Delta l > 0$. For $x \leq l$ the mineral volume fraction vanishes.

The expression for $\Phi_s(x; l)$ is determined as follows (see Eqn. (58)). The time Δt_l for the front to advance from l to $l + \Delta l$ follows from Eqn. (53) by setting the mineral volume fraction evaluated at the position of the front at time $t = t_l + \Delta t_l$ equal to zero according to

$$\phi_s(l + \Delta l, t_l + \Delta t_l) = 0, \tag{54}$$

yielding the expression

$$\Delta t_l = \frac{\Phi_s(l + \Delta l; l) e^{q\Delta l}}{\bar{V}_s k_f \alpha \Delta C_l}. \tag{55}$$

From Eqn. (53), using Eqn. (55), the mineral volume fraction can be written in terms of Δt_l as follows:

$$\phi_s(x, t) = \Phi_s(x; l) - \Phi_s(l + \Delta l; l)\left(\frac{t - t_l}{\Delta t_l}\right) e^{-q(x-l-\Delta l)}. \tag{56}$$

From this result it follows that $\Phi_s(x; l)$ satisfies the recursion relation

$$\Phi_s(x; l + \Delta l) = \Phi_s(x; l) - \Phi_s(l + \Delta l; l) e^{-q(x-l-\Delta l)}, \tag{57}$$

obtained by evaluating Eqn. (56) at $t = t_l + \Delta t_l$ and noting that $\Phi_s(x; l + \Delta l) = \phi_s(x, t_l + \Delta t_l)$ by definition because $t_{l+\Delta l} = t_l + \Delta t_l$. By direct substitution it can be verified that the exact solution to this equation satisfying Eqn. (45) is given by

$$\Phi_s(x; l) = \phi_s^\infty (1 - e^{-q(x-l)}). \tag{58}$$

With this result it is possible to obtain an expression for the velocity of the front by computing the time Δt required for the front to advance through a distance Δl. The velocity v_l is given by the ratio $\Delta l / \Delta t$ in the limit as $\Delta t \to 0$. From Eqn. (58) it follows that

$$\Phi_s(l + \Delta l, l) = \phi_s^\infty (1 - e^{-q\Delta l}),$$
$$\approx \phi_s^\infty q \Delta l, \tag{59}$$

to first order in Δl. Substituting this result into Eqn. (55), the velocity of the front v_l can be expressed according to

$$v_l = \frac{dl}{dt} = \lim_{\Delta t_l \to 0} \frac{\Delta l}{\Delta t_l},$$
$$= \frac{1}{\tau_0 q} \frac{\Delta C_l}{\Delta C_0}. \tag{60}$$

The ratio $\Delta C_l / \Delta C_0$ can be evaluated from the explicit forms for the stationary state corresponding to pure advection (Eqn. (III.8)), pure diffusion (Eqn. (III.5)) and combined advection-diffusion (Eqn. (III.1)) given in Appendix II, resulting in the expressions:

$$\frac{\Delta C_l}{\Delta C_0} = \begin{cases} 1 & (D = 0, v \neq 0) \quad \text{(61a)} \\ \dfrac{1}{ql + 1} & (D \neq 0, v = 0), \quad \text{(61b)} \\ \dfrac{\omega_l}{(\omega_l + 1)} & (D \neq 0, v \neq 0) \quad \text{(61c)} \end{cases}$$

where ω_l is defined by

$$\omega_l = \frac{u}{qD} \frac{1}{1 - e^{-ul/D}}, \tag{62}$$

$u = v/\phi$, and the appropriate expression for q is given by Eqn. (48a), (48b) or (48c), respectively.

Advection. For pure advection the velocity of the front is given by

$$v_l = \frac{1}{\tau_0 q},$$
$$= u\left(\frac{\phi \Delta C_0}{\phi_s^\infty \bar{V}_s^{-1}}\right), \tag{63}$$

as follows from Eqns. (60) and (61a) with q given by Eqn. (48a). According to this expression, the velocity of propagation of the front for surface controlled dissolution given by linear kinetics is independent of the rate constant and surface area of the reacting mineral. Surprisingly, this result is identical with the expression obtained for the velocity of the front in the local equilibrium approximation given by Eqn. (I.6) for $K_d \gg 1$, where K_d is defined in Eqn. (I.7). A similar result has been obtained by ORTOLEVA *et al.* (1986) for the propagation of a redox front based on the traveling wave approximation (see Appendix IV). This approximation is limited to advective dominated systems.

Diffusion. For pure diffusion it follows from Eqns. (60) and (61b) with q given by Eqn. (48b) that

$$v_l = \frac{dl}{dt} = \frac{1}{(ql+1)q\tau_0} \approx \frac{1}{lq^2\tau_0}, \tag{64}$$

where the approximate form holds for $ql \gg 1$. Integrating this expression with the initial condition

$$l(\tau_0) = 0, \tag{65}$$

gives the result

$$l + \frac{1}{2}ql^2 = \frac{1}{q\tau_0}(t - \tau_0). \tag{66}$$

For $ql \gg 1$, the first term on the left-hand side is negligible compared to the second term, and this expression reduces to the familiar result

$$l(t) = 2\Gamma\sqrt{D(t-\tau_0)}, \tag{67}$$

with

$$\Gamma = \frac{1}{q(2\tau_0)^{1/2}} = \left[\frac{\phi\Delta C_0}{2\phi_s^\infty \bar{V}_s^{-1}}\right]^{1/2}. \tag{68}$$

The expression on the right-hand side is just the local equilibrium result for the condition that $\Gamma \gg 1$ (WEARE *et al.*, 1976; LICHTNER *et al.*, 1986a). Thus in this case and for $ql \gg 1$, the rate constant and surface area cancel in the expression for the velocity of the front yielding the local equilibrium result. On the other hand, for $ql \ll 1$ the position of the reaction front is a linear function of time and furthermore, in this case, the velocity of the front depends on the rate constant and surface area.

Combined advection-diffusion. For combined advection-diffusion the situation is more complicated. The velocity of the front can be expressed in the form

$$v_l = \frac{1}{q\tau_0}\frac{\omega_l}{\omega_l + 1}, \tag{69}$$

as follows from Eqns. (60) and (61c) with q given by Eqn. (48c). In this case the product $q\tau_0$ is, in general, a function of the rate constant and surface area, as is ω_l according to Eqn. (62). Thus the velocity of the front, in general, depends on kinetics. From this relation the retardation of the front R_l, defined as the ratio of solute velocity to the velocity of the front, can be expressed according to

$$R_l = \frac{v}{\phi v_l} = K_d(1 - \chi(\eta)e^{-ul/D}), \tag{70}$$

where the function $\chi(\eta)$ is defined by

$$\chi(\eta) = \frac{1}{\eta}(\sqrt{1+\eta} - 1)^2, \tag{71}$$

with the dimensionless variable η defined by

$$\eta = \frac{4k_f\alpha D}{\phi u^2}, \tag{72}$$

and K_d denotes the local equilibrium distribution coefficient defined in Eqn. (I.7). This result is obtained by substituting Eqns. (40), (48c), (49), and (62) into Eqn. (69) and making use of the definition of the retardation factor given in Eqn. (I.5). As is apparent from Eqn. (70) and Fig. 4a, the retardation factor R_l in general depends on the rate constant and surface area. However, R_l exponentially approaches the local equilibrium result as the position of the front l increases, regardless of the value of the parameter η. The factor $\chi(\eta)$ varies between the values of zero and one as shown in Fig. 4b. For $\eta \ll 1$, $\chi(\eta)$ is proportional to η and very little deviation occurs from the local equilibrium value of the retardation for all l. Maximum deviation occurs for $\eta \gg 1$, in which case $\chi(\eta) \approx 1$. For pure advection ($D = 0$), Eqn. (70) reduces to the local equilibrium retardation factor in agreement with Eqn. (63). In the local equilibrium limit $\eta \to \infty$ and the retardation factor becomes

$$R_l^{eq} = K_d(1 - e^{-ul/D}). \tag{73}$$

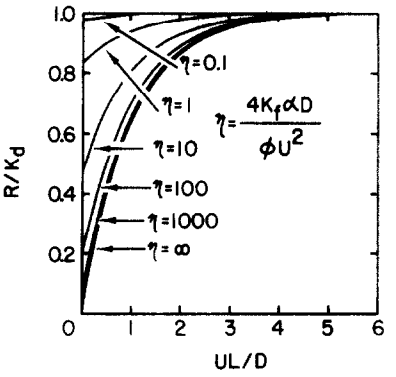

FIG. 4a. A plot of the ratio R_l/K_d where R_l denotes the retardation of the reaction front as predicted by the quasi-stationary state approximation and K_d denotes the local equilibrium distribution coefficient, *versus* the dimensionless variable ul/D. Each curve corresponds to a different value of the dimensionless parameter η defined in Eqn. (72). As the position of the dissolution front denoted by l increases, the retardation factor R_l exponentially approaches the local equilibrium retardation for pure advective transport. The curve labeled $\eta = \infty$ corresponds to the local equilibrium case.

Integrating Eqn. (69) noting that ω_l is a function of l given by Eqn. (62), results in a transcendental equation for $l(t)$ given by

$$\left(\frac{u}{qD} + 1\right)l(t) + \frac{D}{u}\left(\exp\left\{-\frac{ul(t)}{D}\right\} - 1\right) = \frac{u}{q^2D\tau_0}(t - \tau_0). \tag{74a}$$

This equation has two limiting solutions corresponding to diffusion and advection dominated regimes. For $l \ll D/u$, the movement of the reaction front is diffusion dominated and Eqn. (74a) reduces to Eqn. (66) for $u = 0$ and to Eqn. (67) for $ql \gg 1$; for $l \gg D/u$, the motion of the front is dominated by advection and in this case Eqn. (74a) is consistent with Eqn. (63) in the limit as $D \to 0$. Kinetics enters Eqn. (74a) through the factor q and through the characteristic time τ_0. The condition of local equilibrium is obtained in the limit as $k_f\alpha \to \infty$, resulting in the following limiting equation for the position of the reaction front $l_{eq}(t)$:

$$l_{eq}(t) + \frac{D}{u}\left(\exp\left\{-\frac{ul_{eq}(t)}{D}\right\} - 1\right) = \frac{ut}{K_d}, \tag{74b}$$

where the distribution coefficient K_d is given by the limit

$$K_d = \lim_{k_f\alpha\to\infty}\frac{u}{v_l} = \lim_{k_f\alpha\to\infty} q^2D\tau_0 = \frac{\phi_s^\infty \bar{V}_s^{-1}}{\phi\Delta C_0}, \tag{75}$$

in agreement with Eqn. (I.7). This expression is valid for $K_d \gg 1$. It should be emphasized that Eqns. (74a) and (74b) are

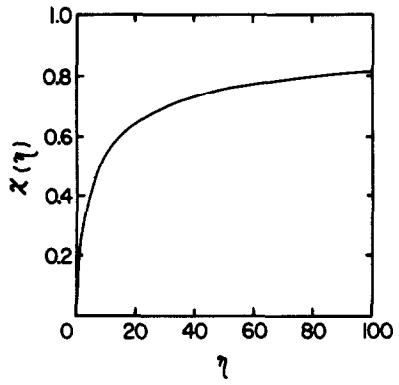

FIG. 4b. The function $\chi(\eta)$ defined in Eqn. (71) plotted as a function of η. Note that $\chi(\infty) = 1$.

exact results within the quasi-stationary state approximation and apply generally to pure diffusion and advection as well as combined advection and diffusion. Equation (74b) can also be obtained directly by integrating the Rankine-Hugoniot equation, Eqn. (I.2), in the quasi-stationary state approximation to the local equilibrium limit of the transport equations.

Although the reaction front velocity is identical in the advection dominated regime for surface and local equilibrium controlled reaction rates the spatial dependencies of the solute concentration, reaction rate and mineral volume fraction are nevertheless qualitatively different. Indeed, in the case of surface controlled reaction, the concentration, reaction rate and mineral volume fraction are piecewise continuous across the reaction front. Hence the Rankine-Hugoniot equation (see Eqn. (I.2)) leads to an indeterminate result for the velocity of the front. As the product of the rate constant and surface area increases, the local equilibrium limit is obtained. In this limit, both the solute concentration and mineral volume fraction contain jump discontinuities across the reaction front, and the reaction rate contains a delta function singularity (LICHTNER *et al.*, 1986a,b). For $x \approx l$ the exponential factor appearing in Eqn. (58) can be replaced by a first order Taylor expansion resulting in an expression for the volume fraction of the form

$$\Phi_s(x;l) = q\phi_s^\infty(x-l) + \cdots. \tag{76}$$

Thus the volume fraction profile near the front depends on the rate constant and surface area. Near the reaction front the mineral volume fraction varies linearly with distance with a slope proportional to q. This suggests the possibility of determining q from field observations of mineral volume fraction profiles.

The position of the reaction front determined from Eqn. (74a) is plotted in Fig. 5 for the dissolution of quartz at 550°C with a diffusion coefficient of 10^{-4} cm^2 sec^{-1}, a Darcy velocity of 1 m year^{-1}, initial volume fraction of quartz equal to 0.9, and a porosity of 10%. The concentration of quartz at the inlet is taken as zero. The rate constant for the dissolution of quartz has the value 10^{-9} moles cm^{-2} sec^{-1} at this temperature. Curves are shown for surface areas corresponding to 0.01, 0.1, 1, and 10 cm^{-1}. The dashed line through the origin corresponds to the local equilibrium result for pure advection. Note that all curves become parallel to the local equilibrium case for sufficiently large times in agreement with Eqn. (73). The early time behavior is diffusion dominated and the effect of advection is unimportant on the position of the dissolution front. Each curve is shifted from the origin by its corresponding delay time τ_0.

There does not exist an analytical solution to the transient formulation of the mass conservation equations for transport by combined advection and diffusion for the moving boundary problem, either in the local equilibrium limit or for surface controlled dissolution. Therefore to test the quasi-stationary state approximation, the exact, transient mass transport equations given by Eqns. (34) and (35) with the reaction rate given by Eqn. (38) must be solved numerically. The numerical finite difference methods outlined in LICHTNER (1985) and LICHTNER *et al.* (1986b) can be used for such purposes. The results obtained are indistinguishable from the curves in Fig. 5 indicating that indeed, the quasi-stationary state approximation is an excellent approximation to the transient mass conservation equations. Furthermore, the curve corresponding to a surface area of 10 cm^{-1} approximates the local equilibrium result, also obtained numerically by solving Eqn. (34) combined with the mass action equation given in Eqn. (I.1).

Numerical solution

There are several factors which may act to alter the stationary state before complete dissolution of the mineral occurs that are not accounted for in the analytical solution presented above. These include changes in surface area of the dissolving mineral grains, and changes in porosity and permeability of the porous medium. As noted above, for pure advection a change in porosity alone does not change the stationary state, according to Eqn. (20). However, if the permeability is altered, then the flow rate v must change thereby altering the stationary state. Only the effect of varying surface area on the stationary state is considered in what follows.

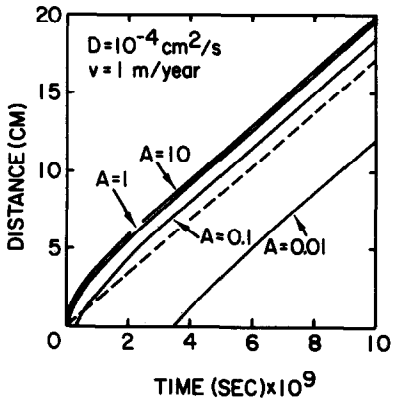

FIG. 5. The position of the quartz dissolution front as a function of time at a temperature of 550°C obtained by numerically solving Eqn. (74a) for $l(t)$ for different surface areas as indicated in the figure. A Darcy velocity of 1 m year^{-1}, diffusion coefficient of 10^{-4} cm^2 sec^{-1}, a rate constant of 10^{-9} moles cm^{-2} sec^{-1}, zero initial concentration of solute species A, and an initial volume fraction of A, of 0.9 were used in the calculation. All curves eventually become parallel to the local equilibrium result for pure advective transport indicated by the dashed line through the origin. The curves are displaced by the time τ_0 required for quartz to completely dissolve at the inlet, which determines the time of initial appearance of the reaction front.

If the surface area of mineral A_s changes as a consequence of chemical reaction, an analytical solution to the stationary state equations no longer exists and numerical techniques must be used. The solute concentration, reaction rate, mineral volume fraction and position of the reaction front are obtained at a discrete set of times corresponding to distinct stationary states. The essential difference between variable and constant surface area is that in the former case the position of the reaction front need not change from one stationary state to the next as was the case for the exact solution presented above. The spatial variation of the surface area, however, is different for different stationary states.

A finite difference approximation to the stationary state equations represents the solute concentration by a discrete set of values C_n^k where the subscript n refers to the nth node point $x_n = n\Delta x$, and Δx designates the spacing between node points. Usual finite difference algorithms can be used to obtain the stationary states C_n^k, as discussed in detail below for pure advection and for combined advection and diffusion, of which pure diffusion is a special case.

Pure advective transport: Lagrangian reference frame—For pure advection the mass transport equation corresponding to the kth stationary state is given by

$$v\frac{dC^k}{dx} = -\frac{\partial \Xi_s^k}{\partial t}(x; l_k), \tag{77}$$

for a fixed position of the dissolution front designated by l_k. In the case of variable surface area, for distinct stationary states κ_1 and κ_2, it is possible that $l_{\kappa_1} = l_{\kappa_2}$. The multiple reaction path formulation of the quasi-stationary state approximation corresponds to introducing a Lagrangian reference frame letting $x = vt'/\phi$. The notation t' is used to distinguish the time of a Lagrangian fluid packet from the time t specifying the evolution of the system at a fixed point in space. Substituting t' for x in Eqn. (77) gives

$$\phi\frac{dC^k}{dt'} = -\frac{\partial \Xi_s^k}{\partial t}(t'; l_k). \tag{78}$$

Either form of the stationary state equations may be solved using standard finite difference techniques. Replacing the time derivative in the Lagrangian formulation by its finite difference form one obtains the finite difference analogue

$$\phi\frac{C_{m+1}^k - C_m^k}{\Delta t'} = \lambda\left(\frac{\partial \Xi_s^k}{\partial t}\right)_{m+1} + (1-\lambda)\left(\frac{\partial \Xi_s^k}{\partial t}\right)_m, \tag{79}$$

where the subscripts $m+1$, m refer to times t'_{m+1} and t'_m respectively, differing by time step $\Delta t'$:

$$t'_{m+1} = t'_m + \Delta t', \tag{80}$$

with $m = 0, 1, 2, \ldots$. The mth node point x_m is associated with time t'_m by Eqn. (22), $x_m = vt'_m/\phi$. For $m = 0$, $t'_0 = 0$ and $C_0^k = C_0$, where C_0 denotes the concentration at the inlet to the porous medium. Values of λ in the range $0 < \lambda \le 1$ correspond to the implicit, and $\lambda = 0$ to the explicit finite difference algorithm. The value $\lambda = 1$ is referred to as the fully backward implicit finite difference algorithm, and $\lambda = \frac{1}{2}$ corresponds to the Crank-Nicholson algorithm.

With the reaction rate for the kth reaction path $\partial \Xi_s^k/\partial t$ given by Eqn. (38), the following recursion relation for the solute concentration is obtained:

$$C_{m+1}^k = C_{eq} - \sigma_{km}(C_{eq} - C_m^k), \tag{81}$$

where the coefficient σ_{km} is defined by

$$\sigma_{km}(\lambda, \Delta t') = \begin{cases} \dfrac{1-(1-\lambda)\Delta t'/\tau_{km}}{1+\lambda\Delta t'/\tau_{km}} & (x \ge l_k) \\ 1 & (x < l_k) \end{cases}, \tag{82}$$

with the characteristic time τ_{km} defined by

$$\tau_{km} = \frac{\phi}{k_f \alpha_{km}}, \tag{83}$$

where α_{km} denotes the surface area at the mth time step corresponding to the kth stationary state. The surface area is assumed to be a function of the mineral volume fraction ϕ_s according to Eqn. (18).

For constant surface area, the solution to the recursion relation C_m^k must agree with the results previously obtained for the exact solution. In this case the characteristic time τ_{km} is independent of both indices k and m and denoted by τ_R (see Eqn. (II.12) in Appendix II). It follows that the quantity $\sigma_{km} = \sigma_k$ depends only on the index k through l_k and not on m. As a consequence, the recursion relation Eqn. (81) can be solved analytically to give

$$C_m^k = C_{eq} - (\sigma_k)^m(C_{eq} - C_0). \tag{84}$$

This result can be compared with the exact solution for constant surface area given by Eqn. (47) or Eqn. (III.8). Expressed in terms of the time along the flow path corresponding to the Lagrangian reference frame, Eqn. (47) yields for $t' \ge \phi l_k/v$:

$$C(t'; l_k) = C_{eq} - e^{-(t'-\phi l_k/v)/\tau_R}(C_{eq} - C_0) \quad (t' > \phi l_k/v). \tag{85}$$

For $t' \le \phi l_k/v$ the concentration is constant and equal to its value at the inlet

$$C(t'; l_k) = C_0 \quad (t' \le \phi l_k/v). \tag{86}$$

According to the finite difference result, in the absence of chemical reaction, $\sigma_k = 1$ and Eqn. (84) yields

$$C_m^k = C_0 \quad (\text{all } m), \tag{87}$$

in agreement with Eqn. (86). When reaction occurs, the two results agree provided

$$\sigma_k(\lambda, \Delta t') \approx e^{-\Delta t'/\tau_R}, \tag{88}$$

by comparing Eqn. (84) with Eqn. (85). Expanding $\sigma_k(\lambda, \Delta t')$ in a Taylor expansion gives to third order in $\Delta t'$

$$\sigma_k = 1 - \frac{\Delta t'}{\tau_R} + \lambda\left(\frac{\Delta t'}{\tau_R}\right)^2 - 6\lambda^2\left(\frac{\Delta t'}{\tau_R}\right)^3 + \cdots. \tag{89}$$

Comparing this expansion with the expansion of the exponential function

$$e^{-\Delta t'/\tau_R} \approx 1 - \frac{\Delta t'}{\tau_R} + \frac{1}{2!}\left(\frac{\Delta t'}{\tau_R}\right)^2 - \frac{1}{3!}\left(\frac{\Delta t'}{\tau_R}\right)^3 + \cdots, \tag{90}$$

demonstrates that $\lambda = \frac{1}{2}$ gives results that are exact to second order in $\Delta t'$, while the explicit ($\lambda = 0$) and fully backward implicit ($\lambda = 1$) finite difference algorithms are only exact to first order.

For variable surface area the finite difference equations for the solute concentration must be solved numerically. According to Eqn. (82), $\sigma_{km} \le 1$ and therefore the finite difference equations always possess a solution. To ensure that the solution is stable and no oscillations occur, it is necessary and sufficient that $\sigma_{km} > 0$, resulting in the following restriction on the size of the time step $\Delta t'$

$$\Delta t' < \frac{\tau_{km}}{1-\lambda}. \tag{91}$$

According to this result the fully backward implicit finite difference algorithm is unconditionally stable. Accuracy considerations result in a more stringent requirement on the size of the time step.

To obtain the mineral volume fraction it is necessary to replace the reaction rate appearing in Eqn. (35) with its value averaged over the $n-1$st and nth node points, $\bar{I}_{sn}^k$, defined by

$$\bar{I}_{sn}^k = \frac{1}{2}(I_{sn}^k + I_{s,n-1}^k), \tag{92}$$

where

$$I_{sn}^k = k_f \alpha_{kn}(C_n^k - C_{eq}), \tag{93}$$

according to Eqn. (30). Justification for this is given in Appendix V (see also LICHTNER *et al.*, 1986a). The average mineral volume frac-

tion $\bar{\phi}_{sn}^{k+1}$ associated with the nth node point for $k+1$st reaction path is obtained in terms of the previous path according to the expression

$$\bar{\phi}_{sn}^{k+1} = \bar{\phi}_{sn}^{k} + \bar{V}_s \bar{I}_{sn}^{k} \Delta t_k, \tag{94}$$

where Δt_k designates the time interval separating the two reaction paths. When mineral A_s completely dissolves at a particular node point, the reaction front advances to the next node point. Thus the position of the reaction front l_{k+1} for the $k+1$st stationary state is determined by the equation

$$l_{k+1} = \begin{cases} l_k & \text{if } \bar{\phi}_{s,l_{k+1}}^{k} > 0 \\ l_k + \Delta x & \text{if } \bar{\phi}_{s,l_k}^{k+1} \le 0 \end{cases}. \tag{95}$$

In the latter case the time step is computed to be

$$\Delta t_k = \frac{\bar{\phi}_{s,l_k}^{k}}{\bar{V}_s |\bar{I}_{s,l_k}^{k}|}. \tag{96}$$

Validity of the quasi-stationary state approximation requires that the velocity of the front is greatly retarded compared to the fluid velocity

$$R_f^{eq} \gg 1, \tag{97}$$

or, equivalently, that the solute concentration is much less than the mineral concentration so that

$$\Delta C_0 \ll \frac{\bar{V}_s^{-1} \phi_s^{\infty}}{\phi}. \tag{98}$$

This in turn implies that the time step Δt_k governing the alteration of the mineral A_s is much greater than the time step $\Delta t'$ associated with the motion of a single packet of fluid:

$$\Delta t' \ll \Delta t_k. \tag{99}$$

Indeed, for constant surface area the time required for the reaction front to advance one node point of width Δx, can be approximated by

$$\Delta t_k \approx \frac{\phi R_f^{eq}}{v} \Delta x, \tag{100}$$

as follows from Eqn. (63). Conversely the time step $\Delta t'$ for a fluid packet to advance a distance Δx is given by the equation

$$\Delta t' \approx \frac{\phi \Delta x}{v}. \tag{101}$$

The ratio of the two time steps $\Delta t'$ and Δt_k is given by

$$\frac{\Delta t_k}{\Delta t'} = \phi R_f^{eq} = \frac{\bar{V}_s^{-1} \phi_s^{\infty}}{\Delta C_0}, \tag{102}$$

from which Eqn. (99) follows.

Numerical results for the dissolution of quartz at 550°C for pure advection are presented in Fig. 6 for constant (solid line) and variable (dashed line) surface area. A flow rate of 1 m year^{-1} and a surface area of 10 cm^{-1} are used in the calculation. The remaining parameters are the same as in Fig. 5. The short dashed line through the origin refers to the local equilibrium result. The delay time τ_0 for constant surface area has the value 3.97×10^6 sec according to Eqn. (40). The delay time is increased by a factor of three for the variable surface area case compared to constant surface area consistent with Eqn. (18). For the case of variable surface area the velocity of the front changes rapidly with time at the initial appearance of the front. The two curves become parallel as time increases. These results may also be checked by numerically solving the transient mass conservation equations, yielding indistinguishable results.

Advection-diffusion. The Lagrangian formulation only applies in the absence of diffusion, $D = 0$, because otherwise each fluid packet could not form a closed system within the fluid phase.

To consider the case of advection, diffusion and dispersion, the finite difference analogue of Eqn. (46) is expressed in the form

$$g_1 C'^{k+1}_{n+1} - \beta_{kn} C'^{k+1}_{n} + g_2 C'^{k+1}_{n-1} = 0, \tag{103}$$

where $n = 1, \ldots, N$, and C'^{k}_{n} is defined by

$$C'^{k}_{n} = C^{k}_{n} - C_{eq}, \tag{104}$$

with

$$C'^{k}_{0} = \Delta C_0, \tag{105}$$

and

$$C'^{k}_{N+1} = 0. \tag{106}$$

The coefficients g_1, g_2 and β_{kn} are defined by

$$g_1 = 1 - \frac{u \Delta x}{2D}, \tag{107}$$

$$g_2 = 1 + \frac{u \Delta x}{2D}, \tag{108}$$

and

$$\beta_{kn} = \begin{cases} 2 - \dfrac{k_f \alpha_{kn}}{\phi D} (\Delta x)^2 & (x \ge l_k) \\ 2 & (x < l_k) \end{cases}. \tag{109}$$

These equations determine the kth stationary state with the reaction front located at l_k. They may be expressed in matrix form according to

$$\mathbf{M}_k \mathbf{C}'_{k+1} = \mathbf{b}, \tag{110}$$

where $\mathbf{C}_k$ denotes the column vector

$$\mathbf{C}'_k = (C'^{k}_{1}, \ldots, C'^{k}_{N})^T, \tag{111}$$

$\mathbf{b}$ designates the vector

$$\mathbf{b} = (g_2 \Delta C_0, 0, \ldots, 0)^T, \tag{112}$$

where the superscript T designates the transpose, and the matrix $\mathbf{M}_k$ has the tridiagonal form

$$\mathbf{M}_k = \begin{bmatrix} -\beta_{k1} & g_1 & 0 & 0 & \cdots & 0 \\ g_2 & -\beta_{k2} & g_1 & 0 & \cdots & 0 \\ 0 & g_2 & -\beta_{k3} & 0 & \cdots & 0 \\ & \vdots & & \vdots & \vdots & \\ 0 & \cdots & 0 & g_2 & -\beta_{k,N-1} & g_1 \\ 0 & \cdots & 0 & 0 & g_2 & -\beta_{kN} \end{bmatrix}. \tag{113}$$

Note that the position of the reaction front enters these equations only through the coefficient β_{kn} according to the definition given by Eqn. (109).

From the kth stationary state, the mineral volume fraction corresponding to the $k+1$st stationary state is determined from the relation

$$\phi_{sn}^{k+1} = \phi_{sn}^{k} + \bar{V}_s I_{sn}^{k} \Delta t_k, \tag{114}$$

where Δt_k designates the time step between the kth and $k+1$st stationary state.

Shown in Fig. 7 are the positions of the dissolution front for quartz at 550°C corresponding to pure diffusion (dashed curves) and combined advection and diffusion (solid curves), plotted as a function of time for variable and constant surface area. A flow rate of 1 m year^{-1}, a diffusion coefficient of 10^{-4} cm^2 sec^{-1}, and an initial surface area of 10 cm^{-1} are used in the calculations. With increasing time the solid curves must eventually become parallel to the local equilibrium limit for

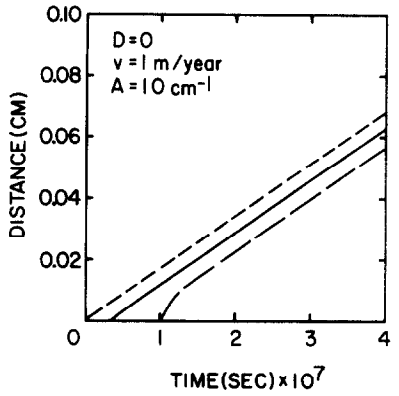

FIG. 6. Position of the reaction front as a function of time for constant (solid curve) and variable (long dashed curve) surface area for pure advection for the system in Fig. 5. The dashed line through the origin corresponds to the local equilibrium result. An initial surface area of 10 cm^{-1}, Darcy flow velocity of 1 m $year^{-1}$, and initial mineral volume fraction of 0.9 were used in the calculation. For the case of variable surface the velocity of the front is initially a function of time, but eventually becomes constant and equal to the local equilibrium result.

pure advection represented by the dashed line through the origin. The curves for variable surface area are shifted from the constant surface area curves resulting from an increase in the delay time τ_0 by a factor of three. These results are consistent with numerical calculations based on the transient mass transport equations.

4. HYDROCHEMICAL WEATHERING OF K-FELDSPAR BY INFILTRATION METASOMATISM

In this section the quasi-stationary state approximation is applied to a simplified description of hydrochemical weathering of a granitic rock consisting of the minerals K-feldspar and quartz. Rainwater is assumed to percolate through the pore spaces of the host rock at a Darcy flow rate of 10 m $year^{-1}$. The calculation presumes that the rate of weathering is controlled by surface reaction of K-feldspar, which dissolves incongruently to form product minerals gibbsite, kaolinite and muscovite. A soil zone, not explicitly incorporated in the calculations, is assumed to lower the pH of the infiltrating rainwater to acidic values. As the host rock becomes weathered in time, a saprolitic zone is formed throughout which most of the K-feldspar is replaced by the minerals gibbsite and kaolinite. Quartz remains essentially unaltered during the weathering process. The calculation is restricted to a single spatial dimension, and no account is taken of changes in permeability and porosity of the weathered saprolite zone which could act to divert the flow of water along the saprolite-fresh rock interface (VELBEL, 1984).

Thermodynamic data for minerals and aqueous species at 25°C and 1 bar are taken from the computer program SUPCRT (see BOWERS *et al.*, 1984, and references therein). The rate constant for quartz is taken from RIMSTIDT and BARNES (1980) and that for K-feldspar from HELGESON *et al.* (1984). Very little data is available for reaction rates of the product minerals gibbsite, kaolinite and muscovite. LASAGA (1984) has given preliminary values for gibbsite and kaolinite. Furthermore, it is difficult to estimate the surface area corresponding to these minerals. In view of this uncertainty, the approach adopted here is to choose values for the product of the rate constant and surface area such that near local equilibrium conditions for precipitation are achieved. A single value for this product of 10^{-14} mole sec^{-1} is used for all three minerals. Values of the equilibrium and rate constants used in the calculation are given in the accompanying table. The composition of the fluid is described by the 5 components K^+, Al^{3+++}, H^+, SiO_2 and Cl^-, an inert species included for charge balance. The initial fluid composition used in the calculation corresponds to a dilute HCl solution with pH 4. The initial composition of the host rock corresponds to a porous arkosic sandstone with volume fractions of 0.2 for K-feldspar and 0.7 for quartz, and a porosity of 10%. The initial surface areas of K-feldspar and quartz are taken as 12 and 40 $cm^2\ cm^{-3}_{rock}$, respectively, and are allowed to vary with reaction according to Eqn. (18).

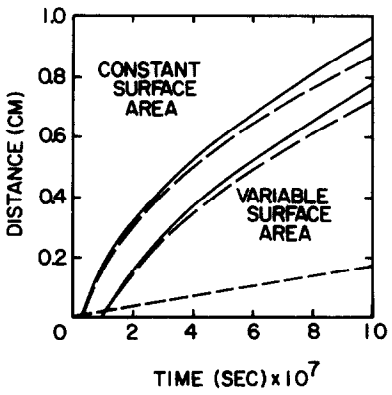

FIG. 7. Position of the reaction front as a function of time for pure diffusion (dashed curve) and combined advection and diffusion (solid curve) for constant and variable surface area. The same parameters are used as in Fig. 5 with an initial surface area of 10 cm^{-1}. The solid curves eventually become parallel to the local equilibrium result for pure advection corresponding to the dashed line through the origin.

TABLE: Reactions accompanying the weathering of K-feldspar in the system K_2O-Al_2O_3-$SiO_{2(aq)}$-HCl-H_2O at 25 °C and 1 bar.

AQUEOUS COMPLEXING REACTIONS	
Reversible Dissociation of Aqueous Species	Log K
$H_2O \rightleftharpoons H^+ + OH^-$	-14.0
$Al(OH)^{++} + H^+ \rightleftharpoons Al^{3+} + H_2O$	4.73
$Al(OH)_4^- + 4H^+ \rightleftharpoons Al^{3+} + 4H_2O$	22.11
$H_3SiO_4^- + H^+ \rightleftharpoons SiO_{2(aq)} + 2H_2O$	9.57

IRREVERSIBLE MINERAL HYDROLYSIS REACTIONS			
Mineral	Irreversible Hydrolysis Reaction	Log k (moles cm^{-2} sec^{-1})	Log K
gibbsite	$Al(OH)_3 + 3H^+ \rightleftharpoons Al^{3+} + 3H_2O$	-14.0	7.96
kaolinite	$Al_2Si_2O_5(OH)_4 + 6H^+ \rightleftharpoons 2Al^{3+} + 2SiO_{2(aq)} + 5H_2O$	-14.0	7.43
muscovite	$KAl_2(AlSi_3O_{10})(OH)_2 + 10H^+ \rightleftharpoons K^+ + 3Al^{3+} + 3SiO_{2(aq)} + 6H_2O$	-14.0	14.56
K-feldspar	$KAlSi_3O_8 + 4H^+ \rightleftharpoons K^+ + Al^{3+} + 3SiO_{2(aq)} + 2H_2O$	-12.65 (pH-dep.) -15.5 (pH-indep.)	0.08
quartz	$SiO_2 \rightleftharpoons SiO_{2(aq)}$	-17.5	-4.0

The time evolution of the weathering process is represented by the sequence of stationary states obtained by numerically solving Eqn. (23) based on the Lagrangian representation of the quasi-stationary state approximation. The reaction rates of the various minerals are shown as a function of distance along the flow path in Fig. 8 for the reaction path corresponding to the first Lagrangian fluid packet. Product minerals gibbsite, kaolinite, and muscovite precipitate from solution as the infiltrating fluid reacts with K-feldspar, forming alteration zones of varying length along the flow path. Gibbsite is the first mineral to precipitate from the packet with an initial zone width less than one meter, followed by kaolinite and muscovite. The spatial overlap between the gibbsite-kaolinite and kaolinite-muscovite zones is a consequence of disequilibrium of the fluid with respect to these minerals. The dissolution rate of K-feldspar is constant over approximately the first 9 meters of the flow path and equal to the far from equilibrium rate of 3.79×10^{-12} moles liter^{-1} sec^{-1}. The rate sharply decreases at the onset of precipitation of muscovite and rapidly approaches equilibrium. The infiltrating fluid reaches quasi-equilibrium with K-feldspar and muscovite within approximately 15 meters of the surface of the host rock. Although muscovite, from its initial onset, continues to precipitate along the entire flow path, its rate of precipitation is so small that it is produced in only infinitesimal quantities.

The lifetime of the first reaction path, and therefore the time of occurrence of the second path, is dependent on the assumption used for computing the change in surface area of the dissolving K-feldspar grains. For constant surface area and assuming a constant fluid flow rate, the positions of the alteration zone boundaries remain stationary with time until K-feldspar completely dissolves at the surface of the host rock. This time, denoted by τ_{Kf}, can be estimated from the equation

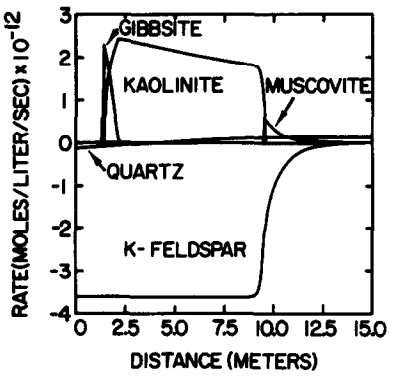

FIG. 8. Reaction rates of reactant and product minerals plotted as a function of distance for the first reaction path resulting from the hydrochemical weathering of K-feldspar and quartz. A dilute HCl solution of pH 4, with a Darcy flow velocity of 10 m year^{-1} infiltrates into the porous rock with an initial porosity of 0.1. See text for a discussion of the parameters used in the calculation. The overlap of the product mineral reaction zones is a consequence of disequilibrium of the reacting minerals with the fluid. The dissolution rate of K-feldspar is constant over the first 9 meters of the flow path. Quartz dissolves along the initial part of the flow path, but precipitates further downstream as a result of the dissolution of K-feldspar. The widths of the reaction zones are directly proportional to the fluid flow velocity and independent of the porosity of the porous medium.

$$\tau_{Kf} \approx \frac{\phi_{Kf}}{\bar{V}_{Kf} k_{Kf} a_{Kf}}, \tag{115}$$

yielding a value of approximately 16,000 years for the parameters given above ($\bar{V}_{Kf}$ = 108.74 cm^3 mole^{-1}). This situation could occur if the decrease in surface area resulting from an overall decrease in grain size, was compensated for by an increase in surface area as a result, for example, of the creation of etch pits with reaction. An alternative possibility resulting in constant surface area is flow in a fracture in which only one surface of the dissolving mineral grains is exposed to the fluid. By taking into account the reduction in surface area of the K-feldspar grains according to Eqn. (18), the product mineral reaction zone boundaries continuously evolve with time. The lifetime of each stationary state in this case is determined by the time required for a significant change to occur in the K-feldspar surface area. As a consequence, the lifetime for the first reaction path is much shorter than that corresponding to constant surface area. It was found that, for the case of variable surface area, 200 year time intervals between stationary states was adequate to obtain convergence.

As shown in Fig. 9 depicting the positions of the reaction zone boundaries as a function of time for times up to 100,000 years, K-feldspar completely dissolves over the initial 9 meters of the host rock after approximately 48,000 years have elapsed, three times the value for constant surface area. The movement of the reaction zones up to this time is entirely a consequence of the change is surface area of the dissolving K-feldspar grains. The gibbsite zone almost completely overlaps the kaolinite zone for times up to approximately 30,000 years. However, as K-feldspar continues to dissolve, a zone consisting of pure gibbsite and quartz several meters wide is formed. As time progresses, both the gibbsite and kaolinite zones continue to grow, the gibbsite at the expense of kaolinite and the kaolinite zone at the expense of K-feldspar. The overlap between the gibbsite-kaolinite zones remains approximately constant. For times greater than 60,000 years the reaction zone boundaries move at constant velocities, indicating formation of a steady-state. The K-feldspar and kaolinite-muscovite boundaries advance at a velocity of approximately 0.57 mm year^{-1}, whereas the downstream gibbsite boundary and the upstream kaolinite boundary advance at a rate of approximately 0.21 mm year^{-1}. The upstream gibbsite boundary moves at a slower rate of approximately 0.077 mm year^{-1}. These rates can be expected to be proportional to the Darcy flow velocity, with a slower velocity resulting in a proportionately slower advancement of the weathered saprolite zone.

The widths of the various reaction zones shown in Fig. 9 are somewhat deceptive because the abundance of each mineral throughout the zone is not indicated. By comparison with Fig. 10a in which the mineral volume fractions and porosity are shown as a function of distance for various times, it is apparent that gibbsite is concentrated over less than half of its total zone width. Muscovite is not produced in sufficient abundance to appear in the figure. Porosity increases throughout the weathered saprolite zone as a result of the negative volume of reaction, consistent with a pseudomorphic replacement mechanism observed in weathered rock. A sharp

weathered-fresh rock interface exists which advances into the host rock with time. Also shown in Fig. 10 are the mineral volume fractions as a function of distance for times corresponding to the steady-state regime. Both the gibbsite and kaolinite zones steadily grow with time as the K-feldspar zone recedes.

The concentration of aqueous species K^+, H^+, SiO_2, and total Al are plotted in Figs. 11a,b,c and d, respectively, as functions of distance for various times indicated in the figures. The potassium ion concentration continuously increases with distance as K-feldspar dissolves. The advance of the K-feldspar boundary is apparent from Fig. 11a, marked by the positions where the concentration of the potassium ion increases from its initial value of 10^{-6} moles liter^{-1}. The pH dramatically increases at the kaolinite-muscovite boundary over a distance of a few centimeters as the fluid approaches equilibrium with K-feldspar. The continuous increase in concentration of SiO_2 is a result of the dissolution of quartz, with the position of the kaolinite boundary marked by a discontinuous change in slope. The sharp increase in the concentration of SiO_2 is a consequence of the dissolution of kaolinite at the beginning of the kaolinite boundary. The total aluminum concentration exhibits a sharp spike coincident with the increase in pH at the kaolinite-muscovite boundary. The movement of the upstream gibbsite zone boundary is apparent in Fig. 11d for times greater than 40,000 years after K-feldspar has completely dissolved, marked by the sudden increase in the total aluminum concentration.

From the change in concentration and mineral volume fraction across a particular reaction front, the velocity of the front, denoted by v_l, can be determined in the steady-state flow regime from the expression

$$v_l = \frac{v}{\phi(1 + L_j)}, \tag{116}$$

with the coefficient L_j defined by

$$L_j = \frac{\sum_{r=1}^{M} \nu_{jr} \bar{V}_r^{-1} \langle \phi_r \rangle}{\phi \langle \Psi_j \rangle}, \tag{117}$$

as demonstrated in Appendix IV. This result is based on the traveling wave approximation (see, *e.g.*, ORTOLEVA *et al.*, 1986, and Appendix IV) and applies to a multi-component system for the case of advective dominated mass transport. The traveling wave approximation requires that the reaction front form a coherent front (HELFFERICH and KLEIN, 1970), in which case L_j is the same for all species. The angular brackets $\langle \cdots \rangle$ denote the difference in the enclosed quantity evaluated at downstream and upstream sides of the front. The expression for the front velocity is formally similar to the corresponding local equilibrium expression with angular brackets replacing square brackets denoting the jump in the enclosed quantity across the reaction front (*cf.* LICHTNER, 1985). The front velocity obtained from Eqn. (116) yields excellent agreement with the corresponding velocities estimated from Fig. 9. For example, referring to Fig. 11a, it follows that $\langle \Psi_{K^+} \rangle \approx 10^{-3.98}$ moles liter^{-1} at the K-feldspar dissolution front. Furthermore, $\phi_{Kf}^{\infty} = 0.2$, and therefore $v_{Kf} \approx 0.57$ mm year^{-1}. Similarly it follows that the velocity of the upstream gibbsite zone boundary is approximately equal to $v_{gibb} \approx 0.074$ mm year^{-1} taking $\phi_{gibb}^{\infty} \approx 0.077$ obtained from Fig. 10 and $\langle \Psi_{Al} \rangle \approx 10^{-4.75}$ according to Fig. 11d, with $\bar{V}_{gibb} = 31.956$ cm^3 mole^{-1}. The velocity of the downstream kaolinite boundary is estimated to be approximately $v_{kaol} \approx 0.25$ mm year^{-1} taking $\langle \Psi_{SiO_2} \rangle \approx 10^{-4.25} - 10^{-5.25} \approx 10^{-4.3}$ with $\phi_{kaol}^{\infty} \approx 0.1$ and $\bar{V}_{kaol} = 99.52$ cm^3 mole^{-1}.

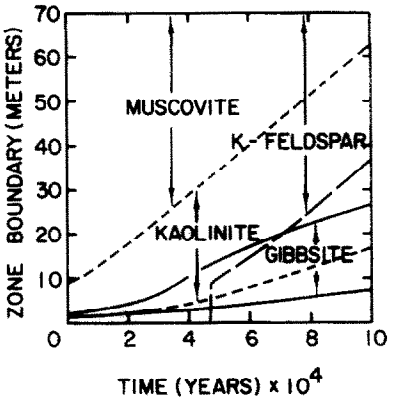

FIG. 9. Position of reaction zone boundaries as a function of time for the hydrochemical weathering of K-feldspar incorporating variable surface area of the dissolving K-feldspar grains. The figure is constructed from a sequence of 500 stationary states each separated by a time interval of 200 years. Parameters used in the calculation are the same as in Fig. 8, depicting the first stationary state. K-feldspar completely dissolves over the first 9 meters of the flow path after approximately 48,000 years have elapsed. For times longer than approximately 60,000 years a steady-state is established in which the reaction zone boundaries move at constant velocities.

To investigate the evolution of the fluid composition along the flow path with time, aqueous concentrations corresponding to stationary states at times t = 200, 2, 3, 4, 5, and 6 $\times 10^4$ years are plotted on an activity diagram in Fig. 12 with x and y axes corresponding to log a_{SiO_2} and log a_{K^+}/a_{H^+}, respectively. Shown in the figure are the stability fields of gibbsite, kaolinite, pyrophyllite, muscovite and K-feldspar. The vertical dashed line indicates the saturation line of quartz. It should be kept in mind that the fluid is generally not in equilibrium with the minerals in the diagram. The sharp bend in the curves at the gibbsite-kaolinite boundary indicates the onset of precipitation of kaolinite. For times greater than 50,000 years, the reaction paths are essentially coincident consistent with the steady-state behavior observed for the reaction zone boundaries in Fig. 9. With increasing time the vertical segment of the reaction paths moves towards the quartz saturation line as the fluid approaches equilibrium with quartz.

Reaction rates of reactant and product minerals for the stationary state corresponding to 50,000 years are shown in Fig. 13 as a function of distance. In similar fashion to the first reaction path, the dissolution rate of K-feldspar decreases sharply at the kaolinite-muscovite boundary and rapidly approaches equilibrium. Muscovite continues to precipitates further downstream, but at an infinitesimal rate. Internal growth within the kaolinite zone is reduced from that of the first path, as a consequence of the decreased dissolution rate of K-feldspar corresponding to a smaller surface area. The behavior of the reaction rates of product minerals shown in the figure is typical for reaction paths subsequent to the first path. The rates of product minerals exhibit sharp peaks cor-

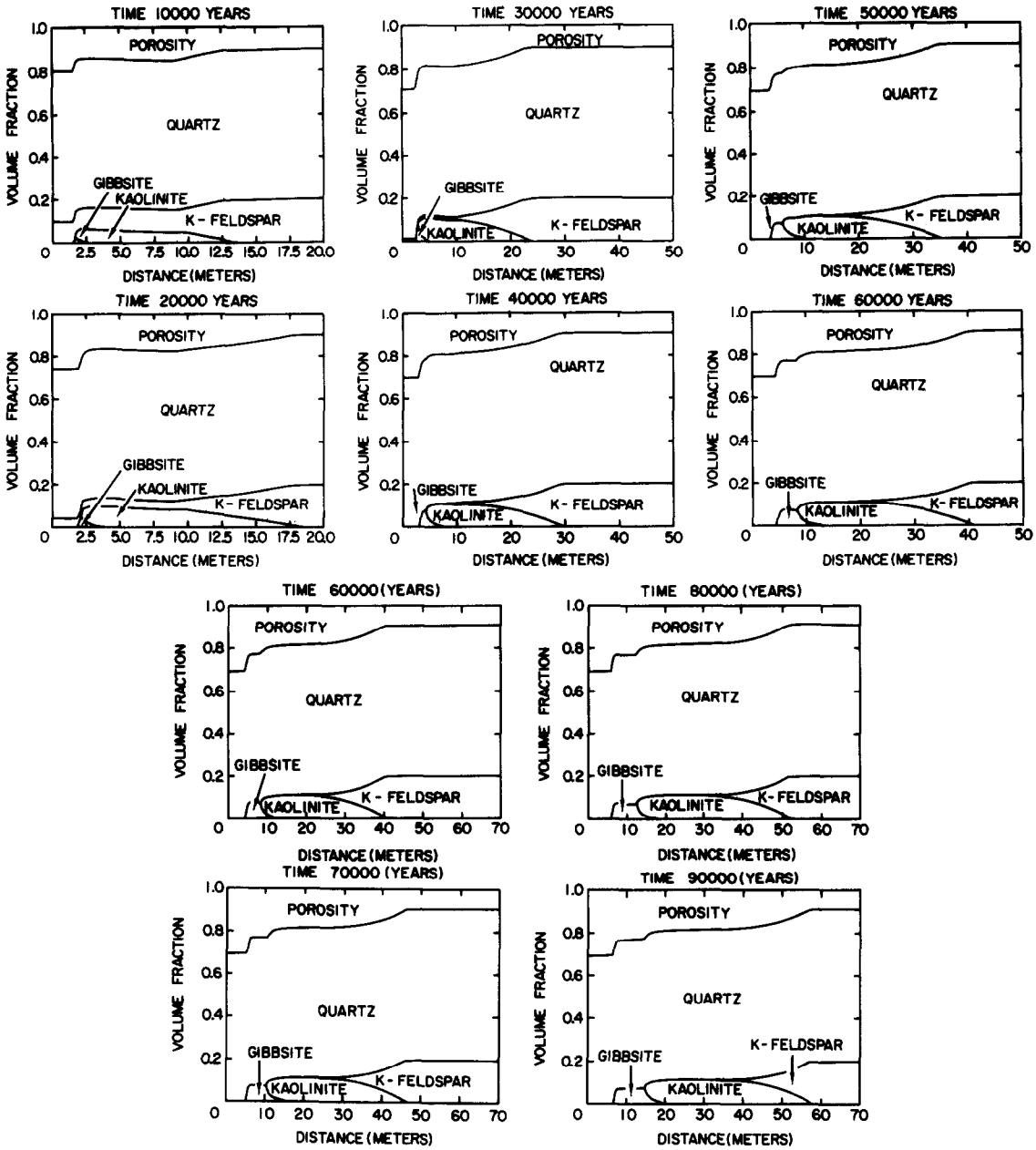

FIG. 10. Volume fractions of the reactant and product minerals and porosity as a function of distance for the indicated times. The same parameters are used as in Fig. 8. Muscovite is produced in too small amounts to appear in the figure. Initially the gibbsite zone is produced directly from the dissolution of K-feldspar. For times greater than 48,000 years after which K-feldspar has completely dissolved throughout the gibbsite zone, the growth of the gibbsite zone results from the dissolution of kaolinite. The kaolinite zone continuously increases in width, growing more rapidly at the expense of K-feldspar than it is converted into gibbsite.

responding to dissolution at the beginning of alteration zones. Gibbsite, kaolinite and muscovite dissolve at their respective upstream boundaries and precipitate further downstream. Coincident with the dissolution of kaolinite, a sharp peak occurs in the rate of gibbsite precipitation that is almost the mirror image of the kaolinite dissolution rate, indicating that gibbsite is forming from kaolinite. A similar behavior occurs downstream where the precipitation rate of kaolinite is the approximate mirror image of the dissolution rate of muscovite, indicating that muscovite is being transformed into kaolinite. This is illustrated in more detail in Fig. 14 where the reaction rates of kaolinite and muscovite are shown as a function of distance. The kaolinite precipitation rate has a sharp peak coincident with the onset of dissolution of muscovite. An increase in the rate constant or surface area of kaolinite, for example, would result in an increase in the height of the peak as its width decreases, approaching a delta function singularity in the limit of local equilibrium. Note that the magnitude of the rates indicate that aluminum is not strictly conserved by the replacement reactions. For ex-

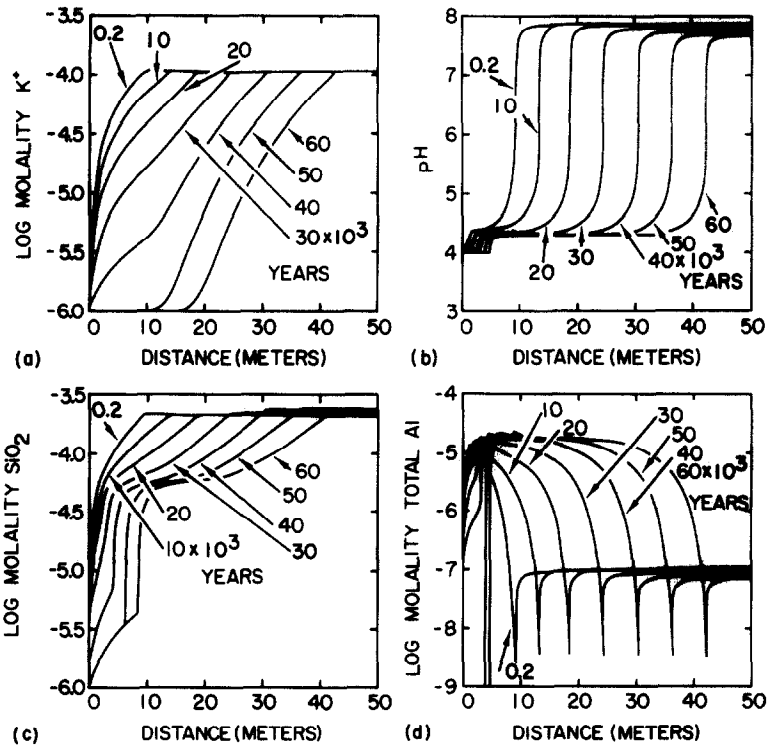

FIG. 11. Aqueous concentration of species K^+, H^+, SiO_2 and total Al plotted as a function of distance for the indicated times. The same parameters are used as in Fig. 8. The position of reaction zone boundaries are visible as discontinuous changes in slope in the concentration profiles.

ample, for the transformation of kaolinite to gibbsite, the rate of gibbsite would need to twice that of kaolinite if aluminum were to be exactly conserved by the reaction.

There has been much discussion in the literature concerning the origin of the gibbsite zone in the genesis of bauxite deposits. To explore in more detail this issue for the calculation described here, the reaction rates of gibbsite and kaolinite are plotted as a function of distance for various times in Fig. 15. For earlier times the gibbsite precipitation rate and kaolinite dissolution rate are not correlated with one another as occurs at later times. Thus, at earlier times gibbsite forms directly from K-feldspar, whereas at later times it forms primarily from the precursor kaolinite. For times later than 48,000 years, the time required for K-feldspar to dissolve completely over the first 9 meters of the flow path, gibbsite forms entirely from kaolinite.

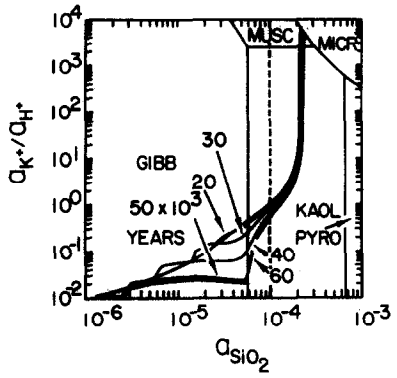

FIG. 12. Plot of reaction paths at the indicated times on an activity diagram. On the vertical axis is plotted the ratio a_{K^+}/a_{H^+} and on the horizontal axis the activity a_{SiO_2}. The paths terminate at equilibrium with muscovite and K-feldspar. For times longer than 60,000 years a steady-state is formed with little change in the reaction path with time. The vertical dashed line denotes saturation of quartz.

5. CONCLUSION

The quasi-stationary state approximation appears to be a powerful, quantitative tool for describing the metasomatic

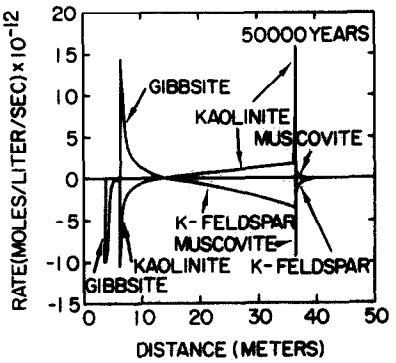

FIG. 13. Reaction rates of reactant and product minerals for the stationary state corresponding to 50,000 years plotted as a function of distance. The behavior is typical for stationary states subsequent to the first. The gibbsite and kaolinite zones dissolve at their respective upstream boundaries and precipitate further downstream. Internal precipitation takes place throughout the kaolinite zone resulting from the dissolution of K-feldspar. A detail of the kaolinite-muscovite boundary is shown in Fig. 14.

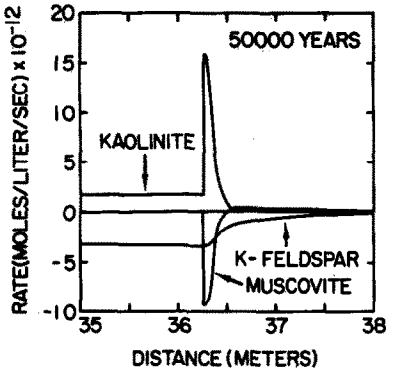

FIG. 14. Detail of the reaction rates of kaolinite and muscovite at 50,000 years plotted as a function of distance in the neighborhood of the kaolinite-muscovite reaction zone boundary. The sharp peak in the precipitation rate of kaolinite coincides with the dissolution of muscovite. Note that aluminum is approximately conserved by the reaction of muscovite + K-feldspar to form kaolinite.

alteration of minerals in response to pure advective, pure diffusive, and combined advective-diffusive mass transport. Within the quasi-stationary state approximation the time evolution of the system is approximated by a sequence of stationary states which quasi-statically adjust to changes in the properties of the host rock. Its validity depends on the rapid formation of a stationary state compared to the time required for significant changes in rock properties. The time for formation of a stationary state is related to the differences in concentration of a species in aqueous solution compared to its concentration in a mineral. Significantly larger time steps can be taken in the numerical integration of the quasi-stationary state equations than is otherwise possible using conventional finite difference algorithms, allowing integration of the governing equations over geologic time spans.

Viewed qualitatively, the quasi-stationary state approximation offers a conceptual understanding of the formation and propagation of mineral alteration zones resulting from surface controlled reaction rates, that is distinct from a local equilibrium chromatographic description. Thus reaction fronts remain stationary in time despite steady fluid flow, unless significant changes in surface area, mineral abundances, porosity or permeability occur to alter the stationary state.

Application of the quasi-stationary state approximation to the dissolution of quartz led to the observation that under certain circumstances the propagation of the quartz dissolution front was independent of the rate constant and surface area and coincided with the local equilibrium limiting behavior. For combined advective-diffusive mass transport the situation was more complicated, but after a sufficiently long period of time had elapsed the local equilibrium front velocity was attained.

Finally, calculations describing the weathering of K-feldspar yielded two distinct processes for the formation of gibbsite. During the initial period of the weathering process gibbsite formed directly from K-feldspar, but at later times it formed indirectly through the precursor kaolinite. Kaolinite formed both directly as a weathering product of K-feldspar and indirectly through the precursor muscovite. While it is difficult to compare these results directly with field observations because of their simplified nature, it is hoped that calculations such as these may form the first step towards more realistic calculations incorporating host rock compositions of greater complexity, as well as two-dimensional fluid flow. For the latter, it is essential to incorporate the change

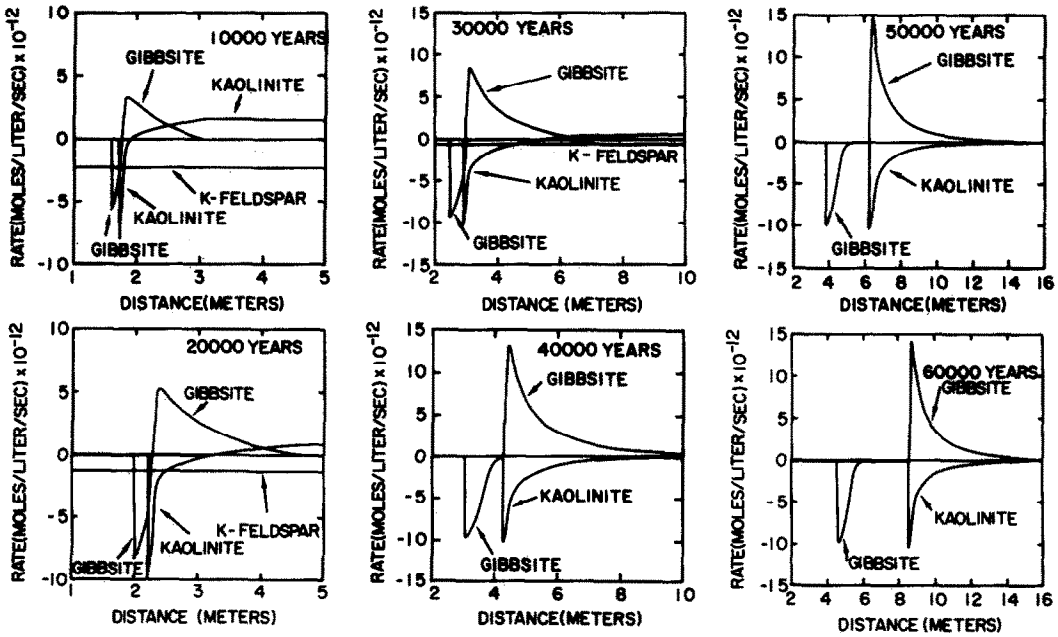

FIG. 15. Reaction rates of gibbsite and kaolinite plotted as a function of distance for various times. During the early periods of the weathering process, gibbsite is produced directly from K-feldspar, whereas at later times it is produced from the dissolution of kaolinite as indicated by the mirror images of the gibbsite and kaolinite rates.

in permeability of the weathered saprolite zone from the almost impermeable host rock.

Acknowledgements—The research described above was supported by Department of Energy (DOE Grants DE-AT03-83ER-13100 and DE-FG03-85ER-13419). Computer calculations were carried out on a CRAY X-MP computer located at the Supercomputer Center, San Diego, California with funding from the National Science Foundation (NSF Grant EAR8115859). I am indebted to Hal Helgeson, Bill Murphy, Eric Oelkers, Barbara Ransom, and Everett Shock for many helpful discussions during the course of this study. I also want to thank Richard Knapp for his thorough and constructive review resulting in a much improved manuscript.

Editorial handling: J. I. Drever

REFERENCES

ARONSSON G. (1985) A new finite element method for estimating the penetration of frost into ground. In *Free Boundary Problems: Applications and Theory* (eds. A. BOSSAVIT, A. DAMLAMIAN and M. FREMOND), Vol. IV, pp. 318–329. Pitman, London.

BEAR J. (1972) *Dynamics of Fluids in Porous Media.* Elsevier, 764p.

BORN M. and HUANG K. (1954) *Dynamical Theory of Crystal Lattices.* Oxford Univ. Press, 420p.

BOWERS T. S., JACKSON K. J. and HELGESON H. C. (1984) *Equilibrium Activity Diagrams for Coexisting Minerals and Aqueous Solutions at Pressures and Temperatures to 5kb and 600°C.* Springer-Verlag, 397p.

CARSLAW H. S. and JAEGER J. C. (1959) *Conduction of Heat in Solids,* 2nd ed. Clarendon Press, Oxford. 510p.

CRANK J. (1984) *Free and Moving Boundary Problems.* Oxford Univ. Press, 425p.

DENBIGH K. G. (1951) *The Thermodynamics of the Steady State.* Methuen, London, 103p.

DOBROVOLSKY, E. V. (1987) Physico-chemical mechanisms of weathering processes and corresponding models of dynamics of mineral zonality evolution. *Chem. Geol.* **60,** 89–94.

FRANTZ J. D. and MAO H. K. (1976) Bimetasomatism resulting from intergranular diffusion: I. A theoretical model for monomineralic reaction zone sequences. *Amer. J. Sci.* **276,** 817–840.

FRANTZ J. D. and MAO H. K. (1979) Bimetasomatism resulting from intergranular diffusion: II. Prediction of multimineralic zone sequences. *Amer. J. Sci.* **279,** 302–323.

HELFFERICH F. and KLEIN G. (1970) *Multicomponent Chromatography.* Marcel Dekker, 419p.

HELGESON H. C. (1968) Evaluation or irreversible reactions in geochemical processes involving minerals and aqueous solutions—I. Thermodynamic relations. *Geochim. Cosmochim. Acta* **32,** 853–877.

HELGESON H. C. and MURPHY W. M. (1983) Calculation of mass transfer among minerals and aqueous solutions as a function of time and surface area in geochemical processes. I. Computational Approach. *Math. Geol.* **15,** 109–130.

HELGESON H. C., MURPHY W. M. and AAGAARD P. (1984) Thermodynamic and kinetic constraints on reaction rates among minerals and aqueous solutions. II. Rate constants, effective surface area, and the hydrolysis of feldspar. *Geochim. Cosmochim. Acta* **48,** 2405–2432.

LASAGA A. C. (1984) Chemical kinetics of water-rock interactions. *J. Geophys. Res.* **89,** 4009–4025.

LICHTNER P. C. (1985) Continuum model for simultaneous chemical reactions and mass transport in hydrothermal systems. *Geochim. Cosmochim. Acta* **49,** 779–800.

LICHTNER P. C. (1987) The method of quasi-stationary states and metasomatism. *European Union of Geosciences,* Strasbourg, France; *Terra cognita* **7,** 408.

LICHTNER P. C., OELKERS E. H. and HELGESON H. C. (1986a) Comparison of numerical finite difference calculations with exact solutions to the moving boundary problem for aqueous diffusion coupled to mineral precipitation/dissolution reactions. *J. Geophys. Res.* **91,** 7531–7544.

LICHTNER P. C., OELKERS E. H. and HELGESON H. C. (1986b) Interdiffusion with multiple precipitation/dissolution reactions: transient model and the steady-state limit. *Geochim. Cosmochim. Acta* **50,** 1951–1966.

LICHTNER P. C., MURPHY W. M. and HELGESON H. C. (1986c) Lagrangian formulation of fluid-rock interaction in flowing systems. *Geol. Soc. Amer. Abstr. Prog.* **18,** 672.

LICHTNER P. C., HELGESON H. C. and MURPHY W. M. (1987) Lagrangian and Eulerian representations of metasomatic alteration of minerals. In *Proc. NATO Advanced Study Institute on Chemical Transport in Metasomatic Processes* (ed. H. C. HELGESON), Reidel, Dordrecht, Holland (in press).

LUNARDINI V. I. (1981) *Heat Transfer in Cold Climates.* Van Nostrand Reinhold, 731p.

MURPHY W. M., OELKERS E. H. and LICHTNER P. C. (1987) Surface *versus* diffusion reaction rates of aqueous species in the control of irreversible mineral hydrolysis in geochemical processes (in preparation).

OELKERS E. H. and HELGESON H. C. (1988) Calculation of the thermodynamic and transport properties of aqueous species at high pressures and temperatures: Aqueous tracer diffusion coefficients of ions to 1000°C and 5 kb. *Geochim. Cosmochim. Acta* **52,** 63–85 (this issue).

OGATA A. (1964) Mathematics of dispersion with linear adsorption isotherm. *U.S. Geol. Surv. Prof. Paper 411-H,* 9p.

OGATA A. (1970) Theory of dispersion in a granular medium. *U.S. Geol. Surv. Prof. Paper 411-I,* 34p.

ORTOLEVA P., AUCHMUTY G., CHADAM J., HETTMER J., MERINO E., MOORE C. H. and RIPLEY E. (1986) Redox front propagation and banding modalities. *Physica* **19D,** 334–354.

ORTOLEVA P., MERINO E., MOORE C. and CHADAM J. (1987) Geochemical self-organization I: reaction-transport feedbacks and modeling approach. *Amer. J. Sci.* (in press).

RIMSTIDT J. D. and BARNES H. L. (1980) The kinetics of silica-water reactions. *Geochim. Cosmochim. Acta* **44,** 1683–1699.

RUBINSTEIN L. J. (1971) The Stefan Problem. *Trans. Math. Monographs* **27,** Amer. Math. Soc., Providence, 419p.

SJÖBERG E. L. and RICKARD D. T. (1984) Temperature dependence of calcite dissolution kinetics between 1 and 62°C at pH 2.7 to 8.4 in aqueous solutions. *Geochim. Cosmochim. Acta* **48,** 485–493.

VELBEL M. A. (1984) Hydrochemical constraints of mass balances in forested watersheds of the southern appalachians. In *The Chemistry of Weathering* (ed. J. I. DREVER), pp. 231–247. NATO ASI Series C, Mathematical and Physical Sciences, 149. Reidel.

WEARE J. H., STEPHENS J. R. and EUGSTER H. P. (1976) Diffusion metasomatism and mineral reaction zones: General principles and application to feldspar alteration. *Amer. J. Sci.* **276,** 767–816.

APPENDIX I: LOCAL EQUILIBRIUM APPROXIMATION

The local equilibrium approximation for the dissolution reaction given in Eqn. (29) can be precisely defined as the limit of the surface controlled reaction rate given in Eqn. (30) as the product of the rate constant k_f and surface area α become infinite (*e.g.* LICHTNER, 1985). In this case the reaction rate $\partial\Xi_s/\partial t(x, t)$ becomes an additional unknown quantity to be determined by solving the mass transport equations. The additional equation needed is the mass action equation expressed in the form of an inequality

$$K^{-1} \geq C(x, t), \tag{I.1}$$

where K denotes the equilibrium constant for the reaction as written in Eqn. (29), and a sufficiently dilute aqueous solution is assumed to justify unit activity coefficient. Equality holds when the fluid is saturated with respect to the solid ($\phi_s \neq 0$), and the inequality when the fluid is undersaturated ($\phi_s = 0$). This restriction on the mass action equation combined with Eqn. (36) defines a moving boundary problem for the local equilibrium case. The mineral dissolves at a sharp reaction front which advances with time at a retarded velocity v_l. The velocity of the reaction front v_l is determined from the generalized Rankine-Hugoniot equation specifying conservation of mass

across the front. The frontal velocity v_l is given as the ratio of the jump in flux to the jump in solute and mineral concentration across the front according to the expression (LICHTNER, 1985)

$$v_l = \frac{v[C]}{[\phi C] + [\phi_s]\bar{V}_s^{-1}}, \tag{I.2}$$

valid for pure advective fluid flow, where v denotes the Darcy velocity, and the square brackets [. . .] denotes the jump in the enclosed quantity across the reaction front. For the initial and boundary conditions given by Eqns. (31), (32) and (33), the jump in solute and mineral concentration are given by

$$[C] = C_{eq} - C_0, \tag{I.3}$$

and

$$[\phi_s] = \phi_s^\infty. \tag{I.4}$$

With these results the Rankine-Hugoniot equation results in a retardation factor R_l^{eq} of the front given by

$$R_l^{eq} = \frac{v}{\phi v_l}, \tag{I.5}$$

$$= 1 + K_d, \tag{I.6}$$

where the distribution coefficient K_d is defined by

$$K_d = \frac{\phi_s^\infty \bar{V}_s^{-1}}{\phi(C_{eq} - C_0)}. \tag{I.7}$$

This result is completely analogous to the description of a chromatographic column in which ion-exchange reactions are substituted for mineral dissolution reactions. According to this result the lower the solubility of the mineral, that is the smaller the equilibrium concentration, the greater the retardation of the reaction front. Under most circumstances of geologic interest the mineral concentration is much larger than the equilibrium aqueous concentration resulting in the inequality

$$C_{eq} \ll \frac{\phi_s^\infty}{\phi \bar{V}_s}, \tag{I.8}$$

or,

$$K_d \gg 1. \tag{I.9}$$

Neglecting changes in porosity and permeability of the porous medium resulting from dissolution of mineral A_s, the solute concentration is given by the expression

$$C(x,t) = \theta(x - l(t))C_{eq} + (1 - \theta(x - l(t))C_0, \tag{I.10}$$

and the mineral volume fraction by

$$\phi_s(x,t) = \theta(x - l(t))\phi_s^\infty, \tag{I.11}$$

where $\theta(x)$ denotes the Heaviside function defined by

$$\theta(x) = \begin{cases} 1 & (x \geq 0) \\ 0 & (x < 0) \end{cases}. \tag{I.12}$$

Substituting Eqn. (I.11) into Eqn. (35) the reaction rate is found to be of the form

$$\frac{\partial \bar{\omega}_s}{\partial t}(x,t) = -\bar{V}_s^{-1}\frac{dl}{dt}\delta(x - l(t)), \tag{I.13}$$

where $\delta(x)$ denotes the Dirac delta function defined by

$$\delta(x) = \frac{d\theta}{dx}(x). \tag{I.14}$$

Thus the concentration and mineral volume both contain jump discontinuities across the reaction front. The rate of dissolution is singular at the front, proportional to the Dirac delta function. This behavior is characteristic of a chemical shock front.

APPENDIX II: TRANSIENT SOLUTION TO THE ADVECTION-DIFFUSION-REACTION EQUATION AND THE STATIONARY STATE LIMIT

The advection-diffusion equation coupled to the linear kinetic reaction rate law given by Eqn. (30) admits an analytical solution provided the reacting mineral does not completely dissolve at any point in space. The solution given here has been adopted from OGATA (1964, 1970) who considered the problem of irreversible ion-exchange. With the initial and boundary conditions specified by Eqns. (31) and (33) the following expression is obtained for the solute concentration $C(x, t)$:

$$C(x,t) = C_{eq} - \frac{C_{eq} - C_0}{2}\left\{e^{-qx}\mathrm{erfc}\left[\frac{x - \Lambda ut}{2\sqrt{Dt}}\right] + e^{(1+\Lambda)(ux/2D)}\mathrm{erfc}\left[\frac{x + \Lambda ut}{2\sqrt{Dt}}\right]\right\}, \tag{II.1}$$

where $\mathrm{erfc}(x)$ denotes the complementary error function, the quantity q is defined by

$$q = \frac{u}{2D}(\Lambda - 1), \tag{II.2}$$

where

$$\Lambda = \left[1 + \frac{4k_f \alpha D}{\phi u^2}\right]^{1/2}, \tag{II.3}$$

and u denotes the average pore velocity defined by

$$u = \frac{v}{\phi}. \tag{II.4}$$

The stationary state limiting form of the transient solution is given by the expression

$$C(x) = C_{eq} - (C_{eq} - C_0)e^{-qx}. \tag{II.5}$$

This result follows from Eqn. (II.1) when

$$\mathrm{erfc}\left[\frac{x - \Lambda ut}{2\sqrt{Dt}}\right] \approx 2, \tag{II.6}$$

and

$$e^{(1+\Lambda)(ux/2D)}\mathrm{erfc}\left[\frac{x + \Lambda ut}{2\sqrt{Dt}}\right] \approx 0. \tag{II.7}$$

Therefore, it follows from properties of the error function that a stationary state is established for $t \gg \tau$ where τ is implicitly defined by the quadratic equation

$$\frac{\Lambda u\tau - x}{2\sqrt{D\tau}} \approx 2. \tag{II.8}$$

A value of 2 is chosen for the argument of the error function because $\mathrm{erfc}(-2) = 1.995$, which is within 0.25% of $\mathrm{erfc}(-\infty) = 2$. At the inlet to the porous medium, $x = 0$, $\tau(x, D, u, \phi, k_f, \alpha)$ is given by the simple expression

$$\tau = 16\frac{D}{\Lambda^2 u^2}. \tag{II.9}$$

Noting that Λ may be expressed in the form

$$\Lambda^2 = 1 + 4\frac{\tau_T}{\tau_R}, \tag{II.10}$$

where the characteristic transport and reaction times, τ_T and τ_R are defined respectively by

$$\tau_T = \frac{D}{u^2}, \tag{II.11}$$

and

$$\tau_R = \frac{\phi}{k_f \alpha}, \tag{II.12}$$

τ has the limiting values

$$\tau = \begin{cases} 16\tau_T & (\tau_R \gg \tau_T) \\ 4\tau_R & (\tau_R \ll \tau_T) \end{cases}. \tag{II.13}$$

Thus two limiting cases exist depending on the relation between τ_T and τ_R.

For pure diffusion ($v = 0$) Eqn. (II.1) reduces to

$$C(x,t) = C_{eq} - \frac{1}{2}(C_{eq} - C_0)\left\{e^{-qx}\mathrm{erfc}\left[\frac{x - 2Dqt}{2\sqrt{Dt}}\right] + e^{qx}\mathrm{erfc}\left[\frac{x + 2Dqt}{2\sqrt{Dt}}\right]\right\}, \quad \text{(II.14)}$$

where

$$q = \sqrt{\frac{k_f \alpha}{\phi D}}. \quad \text{(II.15)}$$

Steady state is reached when $t \gg 4\tau_R$.

For the case of pure advection ($D = 0$) the solute concentration is given by the expression

$$C(x,t) = C_{eq} - (C_{eq} - C_0)e^{-(k_f\alpha/v)x}\theta\left(t - \frac{\phi x}{v}\right). \quad \text{(II.16)}$$

In this case the stationary state limit holds provided $t > \phi x/v$. This is the time required for a packet of fluid to arrive at position x, and therefore the stationary state limit gives the exact result over the region to the left of the infiltration front.

APPENDIX III: STATIONARY STATE SOLUTIONS TO THE ADVECTION-DIFFUSION-REACTION EQUATION

The stationary state solution to the advection-diffusion-reaction equation satisfying the initial and boundary equations given by Eqns. (31) and (33) and continuity conditions at the reaction zone boundary l given by Eqns. (16) and (17) has the form:

$$C(x;l) = \begin{cases} C_0 e^{ux/D} + [C_l - C_0 e^{ul/D}]\dfrac{1 - e^{ux/D}}{1 - e^{ul/D}} & (x \le l) \\ C_{eq} - (C_{eq} - C_l)e^{-q(x-l)} & (x \ge l) \end{cases}, \quad \text{(III.1)}$$

where C_l denotes the concentration at the zone boundary l and q is defined by the expression

$$q = \frac{u}{2D}(\Lambda - 1), \quad \text{(III.2)}$$

and

$$\Lambda = \left[1 + \frac{4k_f\alpha D}{\phi u^2}\right], \quad \text{(III.3)}$$

with $u = v/\phi$. Continuity of the flux at the zone boundary results in the following expression for C_l

$$C_l = \frac{\left(C_{eq} + \dfrac{u}{qD}C_0\right)e^{ul/D} - C_{eq}}{\left(1 + \dfrac{u}{qD}\right)e^{ul/D} - 1}. \quad \text{(III.4)}$$

For pure diffusion the stationary state concentration reduces to the expression

$$C(x;l) = \begin{cases} \dfrac{ql}{ql+1}(C_{eq} - C_0)\dfrac{x}{l} + C_0 & (x \le l) \\ C_{eq} - (C_{eq} - C_l)e^{-q(x-l)} & (x \ge l) \end{cases}, \quad \text{(III.5)}$$

where

$$q = \left(\frac{k_f\alpha}{\phi D}\right)^{1/2}, \quad \text{(III.6)}$$

and

$$C_l = \frac{C_{eq} - C_0}{ql + 1}. \quad \text{(III.7)}$$

Finally for pure advection the stationary state concentration is given by the expression

$$C(x;l) = \begin{cases} C_0 & (x \le l) \\ C_{eq} - (C_{eq} - C_0)e^{-q(x-l)} & (x \ge l) \end{cases}, \quad \text{(III.8)}$$

where

$$q = \frac{k_f\alpha}{v}. \quad \text{(III.9)}$$

APPENDIX IV: THE TRAVELING WAVE APPROXIMATION

In this appendix the traveling wave approximation is used to derive an expression for the velocity of a reaction front for a multi-component, one-dimensional system. It is presumed that one or more reaction fronts exist with the front located at position $l(t)$ propagating with velocity v_l. This approximation assumes that in the neighborhood of each reaction front the solution to the mass transport equations can be represented in the form of a traveling wave given by

$$\Psi_j(x,t) = \Psi_j(x - l(t)), \quad \text{(IV.1a)}$$

and

$$\phi_r(x,t) = \phi_r(x - l(t)), \quad \text{(IV.1b)}$$

for the generalized solute concentration and mineral volume fraction, respectively (ORTOLEVA *et al.*, 1986). Different reaction fronts are assumed to be sufficiently far apart so as not to interact with each other. This form cannot hold when diffusional mass transport is important, as demonstrated below, and therefore the traveling wave approximation is only useful for advective dominated systems.

Combining Eqns. (3) and (4), the transient mass conservation equations for a single spatial dimension can be written in the form

$$\frac{\partial}{\partial t}(\phi\Psi_j + \sum_{r=1}^{M} \nu_{jr}\bar{V}_r^{-1}\phi_r) - \phi D\frac{\partial^2\Psi_j}{\partial^2 x} + v\frac{\partial\Psi_j}{\partial x} = 0. \quad \text{(IV.2)}$$

Representing the generalized concentration Ψ_j and mineral volume fraction ϕ_s by Eqns. (IV.1a,b), and introducing the coordinate x' defined by

$$x' = x - l(t), \quad \text{(IV.3)}$$

Eqn. (IV.2) becomes

$$\frac{d}{dx'}\left\{-\phi D\frac{d\Psi_j}{dx'} + v\Psi_j - v_l(\phi\Psi_j + \sum_{r=1}^{M}\nu_{jr}\bar{V}_r^{-1}\phi_r)\right\} = 0, \quad \text{(IV.4)}$$

where v_l denotes the velocity of the front defined by

$$v_l = \frac{dl}{dt}. \quad \text{(IV.5)}$$

This transformation amounts to choosing a coordinate system at rest with respect to a Lagrangian fluid packet moving with the front. It follows that the quantity in curly brackets must be equal to a constant, or

$$-\phi D\frac{d\Psi_j}{dx'} + v\Psi_j - v_l(\phi\Psi_j + \sum_{r=1}^{M}\nu_{jr}\bar{V}_r^{-1}\phi_r) = \text{constant}. \quad \text{(IV.6)}$$

For the case of pure advective mass transport, evaluating the left hand side of this equation at two distinct points leads to the following expression for the velocity of the front

$$v_l = \frac{v}{\phi R_l}, \quad \text{(IV.7)}$$

where the retardation factor R_l is given by

$$R_l = 1 + L_j, \quad \text{(IV.8)}$$

with the coefficient L_j defined by

$$L_j = \frac{\sum_{r=1}^{M}\nu_{jr}\bar{V}_r^{-1}\langle\phi_r\rangle}{\phi\langle\Psi_j\rangle}. \quad \text{(IV.9)}$$

The angular brackets $\langle\ldots\rangle$ denote the difference in the enclosed quantity at the two chosen points. This result is formally similar to the result obtained in the local equilibrium limit with the angular brackets $\langle\ldots\rangle$ replacing square brackets $[\ldots]$ denoting the jump across the reaction front (*cf.* LICHTNER, 1985, and Appendix I). The traveling wave approximation requires that L_j be the same for all species j, and therefore that $l(t)$ represent a coherent front (HELFERICH and KLEIN, 1970).

It is a simple matter to prove that the traveling wave approximation is not valid when diffusional mass transport is important. If it is valid, then for the single component system discussed in section 3, it follows from Eqn. (IV.6) that

$$-\phi D\frac{dC(x')}{dx'}+vC(x')-v_l(\phi C(x')+\bar{V}_s^{-1}\phi_s(x'))=\text{constant}. \quad \text{(IV.10)}$$

The general solution to the quasi-stationary state equations for either pure diffusion, pure advection, or combined advection and diffusion can be expressed in the form for $x \geq l$:

$$C(x')=C_{eq}-(C_{eq}-C_0)e^{-qx'}, \quad \text{(IV.11a)}$$

and

$$\phi_s(x')=\phi_s^{\infty}(1-e^{-qx'}), \quad \text{(IV.11b)}$$

where $x'=x-l(t)$, and q is given by Eqn. (48). Substituting Eqns. (IV.11a) and (IV.11b) into Eqn. (IV.10), and collecting terms it follows that

$$((v-\phi v_l)C_{eq}+\bar{V}_s^{-1}\phi_s^{\infty})+((\phi Dq+\phi v_l-v)\Delta C_0+v_l\bar{V}_s^{-1}\phi_s^{\infty})e^{-qx'}=\text{constant}, \quad \text{(IV.12)}$$

for all $x' \geq 0$, where ΔC_0 is defined in Eqn. (41). This can only be true if the coefficient multiplying $\exp(-qx')$ is identically zero, resulting in the following expression for the velocity of the front:

$$v_l=\frac{v/\phi-Dq}{1+\bar{V}_s^{-1}\phi_s^{\infty}/\phi\Delta C_0}. \quad \text{(IV.13)}$$

However, Eqn. (IV.13) contradicts the exact results given by Eqn. (64) for pure diffusion, as well as Eqn. (69) for combined advection and diffusion. Thus the travel wave approximation is not valid in these cases.

For pure advection ($D = 0$), Eqn. (IV.13) gives for the retardation factor

$$R_l=1+\frac{\bar{V}_s^{-1}\phi_s^{\infty}}{\phi\Delta C_0}, \quad \text{(IV.14)}$$

in agreement with Eqn. (63) for $R_l \gg 1$. This result also follows directly from Eqn. (IV.9) with

$$\langle C\rangle=C(\infty)-C(0)=C_{eq}-C_0, \quad \text{(IV.15a)}$$

and

$$\langle\phi_s\rangle=\phi_s(\infty)-\phi_x(0)=\phi_s^{\infty}, \quad \text{(IV.15b)}$$

obtained by evaluating the quantities enclosed in the angular brackets asymptotically at $x' = \infty$, and at the reaction front $x' = 0$.

APPENDIX V: LAGRANGIAN REPRESENTATION SPACE AVERAGED REACTION RATE

As demonstrated by LICHTNER *et al.* (1986a) it is necessary to space average the mineral dissolution equation to accurately describe the motion of the reaction front. Writing

$$\bar{\phi}_{s,n+1}(t)=\frac{1}{\Delta x}\int_{x_n}^{x_n+\Delta x}\phi_s(x,t)dx, \quad \text{(V.1)}$$

one obtains

$$\frac{d\bar{\phi}_{s,n+1}}{dt}=\frac{1}{\Delta x}\int_{x_n}^{x_n+\Delta x}\frac{\partial\phi_s}{\partial t}dx,$$

$$=\frac{\bar{V}_x}{\Delta x}\int_{x_n}^{x_n+\Delta x}I_s(x,t)dx, \quad \text{(V.2)}$$

where the reaction rate $I_s(x, t)$ is given by Eqn. (30). Assuming that Δx is sufficiently small so that I_s varies linearly throughout the interval Δx, the reaction rate may be expanded in a Taylor series to first order giving

$$I_s(x,t)=I_s(x_n,t)+\frac{\partial I_s}{\partial x}(x_n,t)(x-x_n), \quad \text{(V.3)}$$

and therefore

$$\int_{x_n}^{x_n+\Delta x}I_s(x,t)dx=\Delta xI_s(x_n+\tfrac{1}{2}\Delta x,t)=\frac{1}{2}\Delta x(I_{sn}+I_{s,n+1}). \quad \text{(V.4)}$$

The average volume fraction $\bar{\phi}_{sn}^{k+1}$ for the k + 1st reaction path is obtained recursively from the expression

$$\bar{\phi}_{sn}^{k+1}=\bar{\phi}_{sn}^{k}+\frac{1}{2}\bar{V}_s(I_{sn}^{k}+I_{s,n-1}^{k})\Delta t_k, \quad \text{(V.5)}$$

obtained by combining the finite difference form of Eqn. (V.2) with Eqn. (V.4), where Δt_k denotes the time step between the kth and k + 1st reaction paths.